Inverse problems in space physics
Part 1: Examples

Bernd Inhester

IMPRS Seminar, May 2002
Draft version

Please report comments, unclear passages, typos, errors to `binhest@linmpi.mpg.de`

1 Introduction

Inverse problem solving has evolved to be a rather mathematical discipline, yet it is intimitely related to observations. The basic goal is to tell how much a measurement can contribute to the validation or falsification of a theoretical model about the object we investigate. In that respect I see it as a very physical discipline: We have to understand both the theoretical model which suggests how the signal we observe is primarily produced and at the same time a detailed knowledge is often required about the instrument which converts the signal into data.

In this first part I will give some examples of inverse problems which show how deeply physics is involved to formulate the problems. The two parts to follow will be concerned with the mathematical tools to solve the problems and we will find that both solvability and solution depend on details of the problem which often can be traced back to its physical nature.

There is a considerable amount of literature which gives an introduction to the topic, others are more of the "cookbook" style and give advice to those who really want to solve a problem. Amoung the first group, I can recommend

> I.J.D. Craig and J.C. Brown, Inverse Problems in Astronomy, Adam Hilger Ltd. Bristol, 1986. (An introduction, we dont have it in our library, but I have a copy)
>
> J.A. Scales and M.L. Smith, Introductory Geophysical Inverse Theory, Samizdat Press, 1997. (freely available in internet: `http://samizdat.mines.edu`)

More comprehensive treatments are

> A. Tarantola, Inverse Problems, Elsevier, 1987. (In the library at [G6 81], a bit old-fashioned)
>
> R. Parker, Geophysical Inverse Theory, Princeton, 1994. (Standard reference for gephysicists, often quoted, should perhaps be bought by the library)

A first aid for practical problem solving is good old

> W.H. Press, B. Flannery, S.A. Teukolsky, W.T. Vetterling, Numerical Recipies, Cambridge University Press, 1986. (The library code is [G6 70]. There are heavily revised more recent editions, the latest version is available in internet: `www.ulib.org/webRoot/Books/Numerical_Recipies`)

A lot of experience in solving inverse problems has been accumulated by geophysicists – so don'nt hesitate to read geophysics books or papers which deal with inverse problems even if you consider yourself an astrophysicist or planetologist.

2 Image deblurring

Green's theorem for the wave equation can be used to calculate the electric wave field $\boldsymbol{E}(\boldsymbol{r},t)$ at any point $\boldsymbol{r}$ inside a closed surface $\mathcal{A}$ if $\boldsymbol{E}$ and its derivative in surface normal direction are known on the surface. For a simple optical telescope, we assume $\mathcal{A}$ to coincide with the aperture plane and $\boldsymbol{E}$ to vanish except on the aperture area A. As aperture, we assume a circular hole of radius R. Then the field behind the aperture is given by an integral only over the aperture area [1].

$$\boldsymbol{E}(\boldsymbol{r},t) = \int_A \boldsymbol{E}(\boldsymbol{r}',t) \frac{\mathrm{e}^{ik|\boldsymbol{r}-\boldsymbol{r}'|}}{ik|\boldsymbol{r}-\boldsymbol{r}'|} \frac{Q}{2\pi}\, d^2(k\boldsymbol{r}') \tag{2.1}$$

Here Q is a directional function depending on the cosines of the angles of the surface normal with $\boldsymbol{r}-\boldsymbol{r}'$ and with the wave vector $\boldsymbol{k}$, respectively. We will consider a telescope with large focal length f so that these angles are close to unity which yields $Q \simeq 1.$ and we can use the Fraunhofer approximation to evaluate the integral (2.1) for some point $\boldsymbol{r}$ on the focal plane. The geometry of the telescope is sketched in Fig. 1. We assume a thin lense immediately in front of the aperture plane which focusses objects at infinity onto the the focal plane.

As a light source, we assume an infinitly distant point source at an angle α from the optical axis. For convenience, we will introduce a separate coordinate system $\boldsymbol{r}_A$ for the vector $\boldsymbol{r}'$ in the aperture plane which originates in the center of the aperture area A. In terms of $\boldsymbol{r}_A$, the wave field in front of the aperture plane and the lense is then given by

$$\boldsymbol{E}'(\boldsymbol{r}',t) = \boldsymbol{E}_0\, \mathrm{e}^{i(\boldsymbol{k}\cdot\boldsymbol{r}' - \omega t)} = \boldsymbol{E}_0\, \mathrm{e}^{i(\boldsymbol{k}_A\cdot\boldsymbol{r}_A - \omega t)} \tag{2.2}$$

where by $\boldsymbol{k}_A$ we denote the projection of $\boldsymbol{k}$ onto the aperture plane. Obviously, the magnitude of $\boldsymbol{k}_A$ is $k \sin\alpha$.

The lense introduces an additional phase retardation on the wave field of $\Delta\phi_{\text{lense}}(\boldsymbol{r}_A) = \Delta\phi_{\text{lense}}(r_A)$ before it reaches the aperture plane. On the aperture plane, the wave field is accordingly given by

$$\boldsymbol{E}(\boldsymbol{r}_A,t) = \boldsymbol{E}_0\, \mathrm{e}^{i(\boldsymbol{k}_A\cdot\boldsymbol{r}_A - \omega t + \Delta\phi_{\text{lense}}(r_A))} \tag{2.3}$$

Similarly as for the aperture plane, we will introduce a similar coordinate system of vectors $\boldsymbol{r}_F$ in the focal plane which originates in the center of the image area F (see Fig. 1). For a point $\boldsymbol{r}$ on the focal plane the distance $\boldsymbol{r}-\boldsymbol{r}'$ can be written in terms of $\boldsymbol{r}_A$ and $\boldsymbol{r}_F$, by $\boldsymbol{r}_F + \boldsymbol{f} - \boldsymbol{r}_A$ where $\boldsymbol{f}$ points from the center of the aperture area A to the center of the image area F. The explicit use of $\boldsymbol{r}_A$ and $\boldsymbol{r}_F$ is helpful because when we approximate the distance according to the ordering $f \gg r_A \gg r_F$.

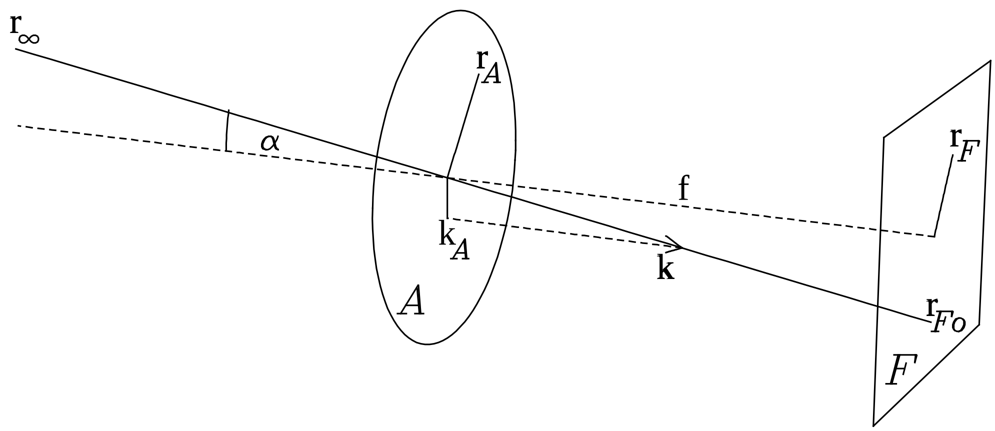

Figure 1: *Geometry for the calculation of the point spread function, $\mathcal{A}$ is the plane of the aperture, $\mathcal{F}$ is the focal plane at a distance f from the aperture. An object is assumed infinitly away in direction of $\boldsymbol{r}_\infty$ and has its geometrical image at $\boldsymbol{r}_{Fo}$ in the focal plane.*

We rewrite (2.1) as

$$\boldsymbol{E}(\boldsymbol{r}_F, t) = \boldsymbol{E}_0 \frac{k\mathrm{e}^{-i\omega t}}{i2\pi f} \int_A \mathrm{e}^{i\Phi(\boldsymbol{r}_F, \boldsymbol{r}_A)} \, d^2(\boldsymbol{r}_A) \tag{2.4}$$

with three contributions to the final phase of the field on the focal plane

$$\Phi(\boldsymbol{r}_F, \boldsymbol{r}_A) = \boldsymbol{k}_A \cdot \boldsymbol{r}_A + \Delta\phi_{\text{lense}}(r_A) + k|\boldsymbol{r}_F + \boldsymbol{f} - \boldsymbol{r}_A| \tag{2.5}$$

These are the initial phase in the aperture plane, the phase retardation due to the lense and the phase change after the propagation from the aperture plane to the focal plane.

The last term in (2.5) can be further approximated with $f \gg r_A \gg r_F$.

$$|\boldsymbol{r}_F + \boldsymbol{f} - \boldsymbol{r}_A| = \sqrt{f^2 + (\boldsymbol{r}_F - \boldsymbol{r}_A)^2}$$
$$\simeq \sqrt{f^2 + r_A^2} \left(1 - \frac{\boldsymbol{r}_F \cdot \boldsymbol{r}_A}{f^2 + r_A^2}\right) \simeq \sqrt{f^2 + r_A^2} - \frac{\boldsymbol{r}_F \cdot \boldsymbol{r}_A}{f}$$

so that (2.5) becomes

$$\begin{aligned}\Phi(\boldsymbol{r}_F, \boldsymbol{r}_A) &= \boldsymbol{k}_A \cdot \boldsymbol{r}_A + \Delta\phi_{\text{lense}}(r_A) + k\sqrt{f^2 + r_A^2} - \frac{k}{f}\boldsymbol{r}_F \cdot \boldsymbol{r}_A \\ &= \frac{k}{f}(\boldsymbol{r}_{Fo} - \boldsymbol{r}_F) \cdot \boldsymbol{r}_A + \Delta\phi_{\text{lense}}(r_A) + k\sqrt{f^2 + r_A^2} \end{aligned} \tag{2.6}$$

$$\text{where} \quad \boldsymbol{r}_{Fo} = \frac{f}{k}\boldsymbol{k}_A$$

is the location of geometric optical image of the distant light source in the focal plane. If we moreover choose

$$\Delta\phi_{\text{lense}} = \phi_0 - \sqrt{f^2 + r_A^2}$$

with arbitray constant ϕ_0, it is easy to see that the phase (2.6) in $\boldsymbol{r}_{Fo}$ is independent on which point $\boldsymbol{r}_A$ the wave field has propagated from and hence all waves interfere coherently in $\boldsymbol{r}_F = \boldsymbol{r}_{Fo}$. This choice therefore insures that plane F is in focus and f is the focal length of the lense.

The final phase in (2.4) therefore is

$$\Phi(\boldsymbol{r}_F, \boldsymbol{r}_A) = \phi_0 - \frac{k}{f}(\boldsymbol{r}_F - \boldsymbol{r}_{Fo})\cdot\boldsymbol{r}_A \tag{2.8}$$

and an evaluation of the phase integral (2.4) now is straight forward. We abbreviate $\boldsymbol{r}_F - \boldsymbol{r}_{Fo} = \Delta\boldsymbol{r}_F$ For a circular aperture area with radius R we have

$$\begin{aligned}
\int_A \mathrm{e}^{i\Phi(\boldsymbol{r}_F, \boldsymbol{r}_A)}\, d^2(\boldsymbol{r}_A) &= \mathrm{e}^{i\phi_0} \int_A \mathrm{e}^{-i\frac{k}{f}\Delta\boldsymbol{r}_F\cdot\boldsymbol{r}_A}\, d^2(\boldsymbol{r}_A) \\
&= \mathrm{e}^{i\phi_0} \int_0^R r_A \underbrace{\int_0^{2\pi} \mathrm{e}^{-i\frac{k}{f}|\Delta\boldsymbol{r}_F|\, r_A\, \cos\varphi}\, d\varphi}_{2\pi \mathrm{J}_0(\frac{k}{f}|\Delta\boldsymbol{r}_F|\, r_A)} dr_A \\
&= 2\pi \left(\frac{f}{k|\Delta\boldsymbol{r}_F|}\right)^2 \mathrm{e}^{i\phi_0} \underbrace{\int_0^{\frac{kR}{f}|\Delta\boldsymbol{r}_F|} \mathrm{J}_0(\rho)\, \rho\, d\rho}_{\frac{kR}{f}|\Delta\boldsymbol{r}_F|\ \mathrm{J}_1(\frac{kR}{f}|\Delta\boldsymbol{r}_F|)} \\
&= 2\pi R^2\, \frac{\mathrm{J}_1(\frac{kR}{f}|\Delta\boldsymbol{r}_F|)}{\frac{kR}{f}|\Delta\boldsymbol{r}_F|}\, \mathrm{e}^{i\phi_0}
\end{aligned} \tag{2.9}$$

The final field is

$$\boldsymbol{E}(\boldsymbol{r}_F, t) = \boldsymbol{E}_0\, \frac{kR^2}{f}\, \frac{\mathrm{J}_1(\frac{kR}{f}|\Delta\boldsymbol{r}_F|)}{\frac{kR}{f}|\Delta\boldsymbol{r}_F|}\, \mathrm{e}^{i(\phi_0 - \frac{\pi}{2} - \omega t)} \tag{2.10}$$

But we are measuring intensities rather than electric wave fields. We therefore square (2.10) and define the power collected from the light source at $\boldsymbol{r}_\infty$ by the aperture area as $P_0 = \pi R^2\, c\boldsymbol{E}_0^2/2$. This power is distributed as on the focal plane as intensity

$$I(\boldsymbol{r}_F) = \frac{c}{2}|\boldsymbol{E}(\boldsymbol{r}_F, t)|^2 = \frac{P_0}{\pi}\left(\frac{kR}{f}\right)^2 \left(\frac{\mathrm{J}_1(\frac{kR}{f}|\Delta\boldsymbol{r}_F|)}{\frac{kR}{f}|\Delta\boldsymbol{r}_F|}\right)^2 \tag{2.11}$$

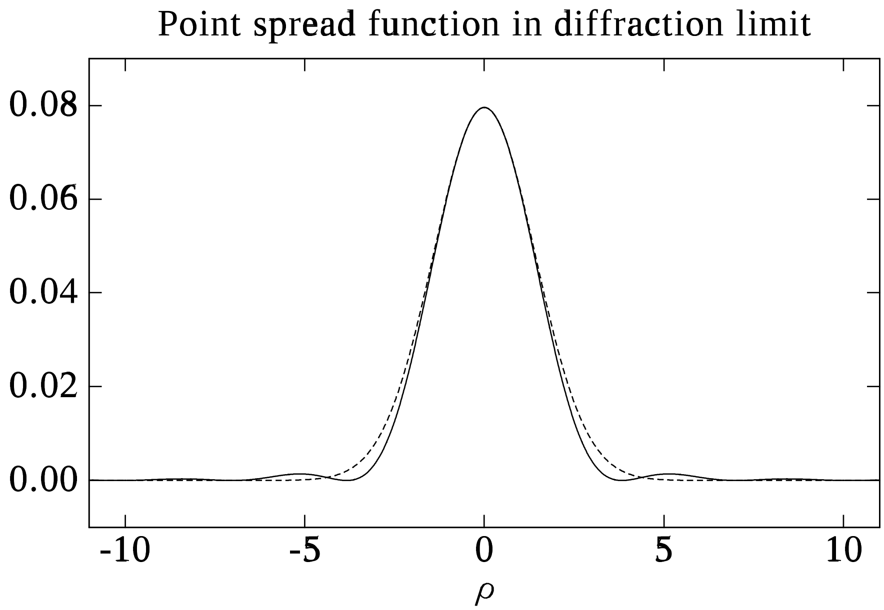

Figure 2: *Cross section through the point spread function* $(1/\pi)(J_1(\rho)/\rho)^2$ *and a Gaussian* $(1/4\pi)\exp-(\rho/2)^2$ *of similar shape (dashed).*

Note that the coefficient of P_0 on the right hand side is normalized and integrating the right hand side over the entire focal plane just yields P_0.

Finally we generalize (2.11) by replacing P_0 for the point source by $I_0(\boldsymbol{r}_{Fo})d^2\boldsymbol{r}_{Fo}$ for a distributed source. The final integral is then

$$\boxed{I(\boldsymbol{r}_F) = \int_F I_0(\boldsymbol{r}_{Fo})\,\frac{1}{\pi}\left(\frac{\mathrm{J}_1(\frac{kR}{f}|\boldsymbol{r}_F - \boldsymbol{r}_{Fo}|)}{\frac{kR}{f}|\boldsymbol{r}_F - \boldsymbol{r}_{Fo}|}\right)^2\left(\frac{kR}{f}\right)^2 d^2\boldsymbol{r}_{Fo}} \tag{2.12}$$

If we know the source distribution $I_0(\boldsymbol{r}_{Fo})$ we can calculate what the observed intensity $I(\boldsymbol{r}_F)$ will look like by simple integration of (2.12). This usually called the forward problem. The equation becomes an inverse problem if we are interested to find out the original intensity distribution $I_0(\boldsymbol{r}_{Fo})$ from the observation $I(\boldsymbol{r}_F)$. This latter problem obviously is of much more practical relevance. More generally, we will call $I(\boldsymbol{r}_F)$ briefly the "data" and $I_0(\boldsymbol{r}_{Fo})$ the "model". The kernel function maps the model to the data and the inverse character of solving for the model lies in the fact that this mapping has to be inverted.

In the present context the kernel function is often called the point spread function and is shown in Fig. 2. For practical calculations, it can well be approximated by a Gaussian. The kernel function in (2.12) depends only on the difference between $\boldsymbol{r}_F$, i.e., the coordinate in data space, and $\boldsymbol{r}_{Fo}$, the coordinate in model space, which makes (2.12) a convolution type integral. It is obvious that the fine structure of $I_0(\boldsymbol{r}_{Fo})$ at scales smaller than about f/kR are lost due to the diffraction of the instrument and there is quite some interest to “deblurr” images in order to resolve these scales.

3 Tomography

The term tomography is used for a variety of methods which all aim to deduce the interior structure of a body from the outside observations. In the mathematical literture this term is used even more generally to denote those problems which derive parameters in the interior of a domain from data taken on its boundary. Here, we will only mention the most prominent examples. Standard references in this area are [3] for a more practical point of view and [2] for the more mathematically interested reader.

3.1 X-ray transform

The classical example of tomography is transmission tomography. Here a diagnostic ray is penetrating the body from various positions and in different directions. The attenuation of the ray as it leaves the body is the data from which the attenuation coefficient κ in the interior is derived. Hence for a position $\boldsymbol{r}_0$ of the transmitter and $\boldsymbol{r}_1$ of the receiver, both connected by a ray path $\mathcal{C}$ through the domain Ω, the initial intensity I_0 is attentuated to

$$I_1(\boldsymbol{r}_0, \boldsymbol{r}_1) = I_0 \exp\left[- \int\limits_{\mathcal{C}(\boldsymbol{r}_0,\boldsymbol{r}_1)\cap\Omega} \kappa(\boldsymbol{r}) \, d\boldsymbol{r} \right] \tag{3.1}$$

To simplify the analysis, the physical nature of the diagnostic ray is often chosen such that the ray path $\mathcal{C}$ is not refracted but straight and the medium is optically thin (this is not always possible as, e.g., in acoustic wave tomography). In this case $\mathcal{C}$ can be characterized by any point $\boldsymbol{r}_0$ on the ray and the ray direction $\boldsymbol{e}_\theta$ as $\mathcal{C} = \{\boldsymbol{r}_0 + s\boldsymbol{e}_\theta \mid s \in \mathbb{R}\}$. Let $s = s_0$ and s_1 correspond to the intersections of $\mathcal{C}$ with the boundary of Ω, then loragrithm of the relative attenuation is

$$\begin{aligned} \ln\left(\frac{I_0 - I_1(\boldsymbol{r}_0, \theta)}{I_0}\right) &= \int_{s_0}^{s_1} \kappa(\boldsymbol{r}_0 + s\boldsymbol{e}_\theta) \, ds \\ = \int\limits_{\Omega} \left[\int_{s_0}^{s_1} \delta(\boldsymbol{r}_0 + s\boldsymbol{e}_\theta - \boldsymbol{r}) \, ds \right] \kappa(\boldsymbol{r}) \, d^3\boldsymbol{r} \end{aligned}$$

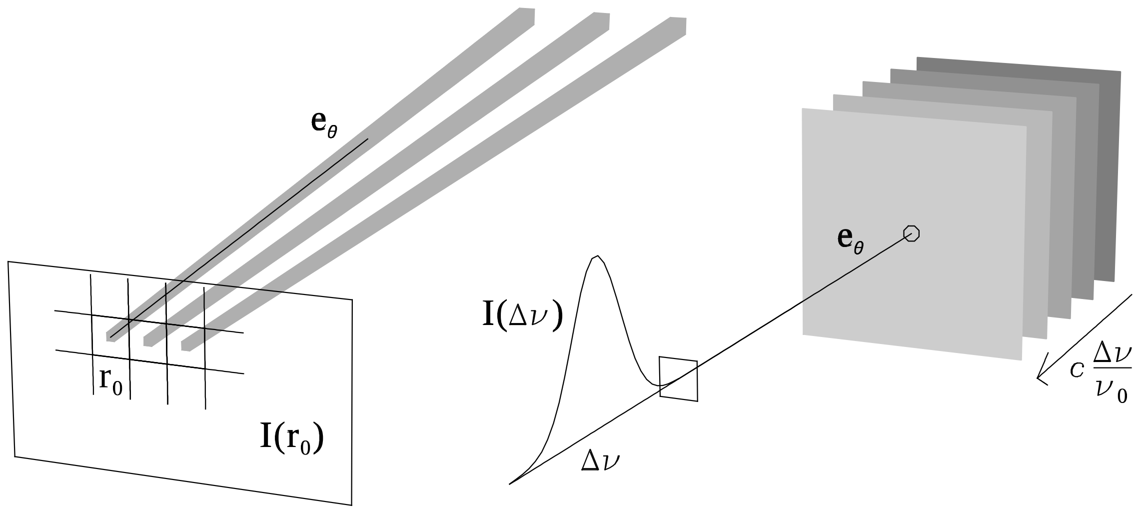

Figure 3: *Illustration of the X-ray transform (left) and the Radon-transform (right) geometry. In both cases the view direction $\boldsymbol{e}_\theta$ is the same. The different integration area is grey-scaled in each case.*

where in the last formulation the kernel function is written out explicitly in the square brackets (by a δ function with vector argument we mean the product of δ functions of the components of the vector argument). In terms of an inverse problem, the logarithm of the relative attenuation $(I_0 - I_1)/I_0$ is the data, and κ the model to be solved for.

(3.1) can also be looked upon as a set of projections of κ along the directions $\boldsymbol{e}_\theta$ onto $\boldsymbol{r}_0$. Up to now, the diagnostic rays have not been specified. To investigate a 3D body, the usual setup is to take a 2D manifold of positions $\boldsymbol{r}_0$ (which make up an image) for a 1D manifold of directions (the scan directions θ must cover $[0, \pi]$, a viewing direction $\boldsymbol{e}_\theta \rightarrow -\boldsymbol{e}_\theta$ gives the integral in 3.1). In this case the (3.1) is called an X-ray transform and the inversion problem is to deduce κ on a 3D domain Ω from a set of 2D images taken at a series of view directions $\boldsymbol{e}_\theta$ (see Fig. 3).

The degree to which (3.1) can be solved depends strongly among other things on the resolution of the image and the selection of view directions. Gaps in the angular coverage or in parts of the image can cause the inverse problem to become unsolvable. A favourable arrangement, on the other hand, is to choose the view directions $\boldsymbol{e}_\theta$ to lie in a plane. Then the 3D X-ray transform decomposes into a set of 2D transforms which can all be solved independently.

The X-ray transform arises also in many other problems which can approximately be linearized. As another example consider the case where the radiation is generated inside the body (a plasma of emitting particles or a radioactive pharmaceutical nuclei in a human body). Then the data in an integral equation formally identical to (3.1) is the observed radiance or intensity and the attenuation κ is replaced by the local emissivity of the radiation. Another case which leads to (3.1) is traveltime tomography. The time a signal needs to propagate from the transmitter to the receiver assuming the propagation takes place along straight lines is

$$T(\boldsymbol{r}_0, \theta) = \int_{s_0}^{s_1} \frac{1}{c(\boldsymbol{r}_0 + s\boldsymbol{e}_\theta)}\, ds \tag{3.2}$$

where c is the local signal speed. To solve (3.2) for the speed c directly would make the problem nonlinear. Instead, (3.2) is usually solved for its reciprocal, the "slowness" $1/c$ (Note, however, that in 3.2 $c(\boldsymbol{r})$ cannot vary by a large amount because then the ray path would be diffracted which invaldates our assumption of straight rays paths). Then (3.2) formally becomes equal to an X-ray transform and c can be determined finally from the recipocal value of the slowness.

3.2 Radon transform

A different transform arises if instead of solving for the spatial variation of a parameter, we want to resolve a distribution in velocity space. Assume we are measuring the line emission from a cloud of plasma from different directions $\boldsymbol{e}_\theta$ without any spatial resolution but rather using a spectrograph to obtain the Doppler shift information from the plasma particles. The intensity at a frequency ν offset from the line center by a shift $\Delta\nu = \nu - \nu_0$ is directly proportional (assuming again the plasma is optically thin) to the number of particles which have a velocity component $v = c\Delta\nu/\nu_0$ towards the observer. Hence,

$$\boxed{I(\Delta\nu, \theta) = \frac{\int I\, d\nu}{N} \int\limits_{\boldsymbol{v}\cdot\boldsymbol{e}_\theta = c\frac{\Delta\nu}{\nu_0}} f(\boldsymbol{v}) d^2\boldsymbol{v}} \tag{3.3}$$

where f is the velocity distribution function, $N = \int f\, d^3\boldsymbol{v}$ is the total number of emitting particles and $\int I\, d\nu$ the integrated line intensity which must be independent of the direction it is measured from.

(3.3) is an example of a Radon transform. For a single view direction $\boldsymbol{e}_\theta$, the integration now is on planes normal to $\boldsymbol{e}_\theta$ rather than on lines along $\boldsymbol{e}_\theta$ as for the X-ray transform (see Fig 3). Each plane is labeled by its distance from the origin which here is proportional to $\Delta\nu$. Therefore, for each direction we only get a 1D manifold of data (the spectrum $I(\Delta\nu)$) and we need a 2D manifold of directions ($\boldsymbol{e}_\theta$ has to cover a half sphere, again replacing $\boldsymbol{e}_\theta \rightarrow -\boldsymbol{e}_\theta$ gives the same spectrum in (3.1) except for a sign change in $\Delta\nu$) to resolve the complete velocity distribution. This is a difficult measurement and (3.3) is therefore often used together with the assumption of some symmetries of the velocity distribution function like, e.g., gyrotropy which means that $f(\boldsymbol{v})$ has azimuthal symmetry with respect to the magnetic field direction.

In a 2D geometry, the X-ray transform and the Radon transform are actually identical except that $\boldsymbol{e}_\theta$ is rotated by $\pi/2$.

4 Radiative transfer inversion problems

Many inverse problems arise from remote sensing observations. The physical basis is the transfer of radiation through media with varying optical properties. In its simplest form, the radiance I_ν at a frequency ν and similarly the background atmosphere have a spatial variation only with height z. Then ignoring scattering, the radiance $I(z, \theta)$ propagating at an angle θ with respect to the vertical $\hat{\boldsymbol{z}}$ is modified locally by absorption and thermal emission according to

$$\frac{d}{d\ell} I_\nu(z,\theta) = \cos\theta \frac{d}{dz} I_\nu(z,\theta) = -\kappa_\nu(z) I_\nu(z,\theta) + \epsilon_\nu \tag{4.1}$$

Here, κ_ν is the local absorption coefficient. A common approximation for the emission source ϵ_ν is a local thermodynamic equilibrium for which it is proportional to Planck's black body radiance of the local temperture $T(z)$

$$\epsilon_\nu = \kappa_\nu(z) B_\nu(T(z)) \quad \text{where} \quad B_\nu(T(z)) = \frac{2h\nu^3}{c^2} \frac{1}{\exp(\frac{h\nu}{k_B T(z)}) - 1} \tag{4.2}$$

The integration of (4.1) is usually simplified by introducing the frequency dependent optical depth

$$\tau_\nu(z) = \int_z^\infty \kappa_\nu(z')\, dz' \quad \text{hence} \quad \kappa_\nu\, dz = -d\tau_\nu \tag{4.3}$$

which starts at zero far above the atmosphere and increases downwards (in opposite direction to z). This changes (4.1) to

$$\begin{aligned} &\cos\theta \frac{d}{d\tau_\nu} I_\nu(\tau_\nu,\theta) = I_\nu(\tau_\nu,\theta) - B_\nu(T(\tau_\nu)) \\ \text{or} \quad &\cos\theta \frac{d}{d\tau_\nu}\left[I_\nu(\tau_\nu,\theta)\, \mathrm{e}^{-\tau_\nu/\cos\theta}\right] = -B_\nu(T(\tau_\nu))\, \mathrm{e}^{-\tau_\nu/\cos\theta} \end{aligned} \tag{4.4}$$

Integration of (4.4) is straight forward except that we have to take account of boundary conditions which typically are different for the case of upgoing radiation

($\theta \in [-\pi/2, \pi/2]$ with $\cos\theta > 0$) and downgoing radiation ($\theta \in [-\pi, -\pi/2] \cup [\pi/2, \pi]$ with $\cos\theta < 0$).

For the case of upgoing radiation we assume a certain radiance $I_\nu^{\rm srf}$ emitted from the surface at z = 0, i.e. where τ_ν attains the value $\tau_\nu^{\rm atm}$ of the optical thickness of the whole atmosphere and a radiance $I_\nu^{\rm spc}$ far above the atmosphere at τ_ν = 0 in space. With these boundary values the integration of (4.4) yields

$$\underbrace{I_\nu \, {\rm e}^{-\tau_\nu/\cos\theta}\Big|_0^{\tau_\nu^{\rm atm}}}_{I_\nu^{\rm srf}\, {\rm e}^{-\tau_\nu^{\rm atm}/\cos\theta} - I_\nu^{\rm spc}} = -\int_0^{\tau_\nu^{\rm atm}} B_\nu(T(\tau_\nu))\, {\rm e}^{-\tau_\nu/\cos\theta} \frac{d\tau_\nu}{\cos\theta}$$

or

$$I_\nu^{\rm spc} = I_\nu^{\rm srf}\, {\rm e}^{-\tau_\nu^{\rm atm}/\cos\theta} + \int_0^{\tau_\nu^{\rm atm}} B_\nu(T(\tau_\nu))\, {\rm e}^{-\tau_\nu/\cos\theta} \frac{d\tau_\nu}{\cos\theta} \qquad (4.5)$$

In the second case of downgoing radiation we assume a the radiance $I_\nu^{\rm srf}$ to reach the surface at z = 0, i.e., at τ_ν = $\tau_\nu^{\rm atm}$ and set the incoming radiance $I_\nu^{\rm spc}$ from above the atmosphere to zero. Then similarly as above (but now $\cos\theta$ is < 0)

$$I_\nu^{\rm srf} = \int_0^{\tau_\nu^{\rm atm}} B_\nu(T(\tau_\nu))\, {\rm e}^{-(\tau_\nu^{\rm atm} - \tau_\nu)/|\cos\theta|} \frac{d\tau_\nu}{|\cos\theta|} \qquad (4.6)$$

4.1 Solar limb darkening

The first case is characteristic for atmospheric observations from space. Another application is the radiative transfer through the solar atmosphere where $I_\nu^{\rm spc}$ ist the radiance of the Sun detected on earth (ignoring modifications by the earth's atmosphere). In the case of the Sun, the surface is not well defined, but it can rather be looked upon as a ball of gas with increasing optical depth towards the interior. A common definition of the photosphere is infact the level where τ_ν = 1 for a certain frequency in the optical spectrum. We can therefore move the level z = 0 deep into the Sun and replace (4.5) by

$$\boxed{I_\nu^{\rm spc}(\cos\theta) = \int_0^{\infty} B_\nu(T(\tau_\nu))\, {\rm e}^{-\tau_\nu/\cos\theta} \frac{d\tau_\nu}{\cos\theta}} \qquad (4.7)$$

This integral equation has been used to infer the variation of $B_\nu(T(\tau_\nu))$ throughout the solar atmosphere from observations of $I_\nu^{\rm spc}(\cos\theta)$, i.e., the brightness of the solar disk with relative distance ρ = $\sqrt{1-\cos^2\theta}$ from the center [7]. From $B_\nu(T(\tau_\nu))$ the temperature variation can then be deduced by inverting (4.2). The kernel of the above inverse problem is the exponential function. Since $\cos\theta$ cannot rise above 1, (4.7) is rather insensitive to $B_\nu(T(\tau_\nu))$ for $\tau_\nu >$ beyond about

1.5 which is natural because we cannot "look" into the optically thick layers and therefore cannot find how they are structured. For $\cos\theta$ close to 0 the kernel drops rapidly with τ_ν and $I_\nu^{\rm spc}$ is an integral over only the uppermost layers with $\tau_\nu \ll 1$. Since the observations this close to the limb are difficult, (4.7) practically can be used only for a range of τ_ν between about 0.1 and 1.5.

For optical frequencies, the brightness drops with $\rho = \sqrt{1-\cos^2\theta}$ (limb darkening) so that qualitatively we expect a decrease of the source function $B_\nu(T(\tau_\nu))$ with decreasing τ_ν, i.e., with increasing height. The related temperature decrease on the Sun occurs from the photosphere to the chromosphere. However, because κ_ν differs with frequency, the sensitive range of τ_ν of the integral kernel in (4.7) relates to different physical height ranges. In fact, observations at UV and EUV frequencies show a limb brightening rather than a darkening indicative of a temperature increase at greater heights. However, at these heights the assumption of local thermodynamic equilibrium which leads to (4.2) is no more valid.

4.2 Trace gas line inversion

An example for the second case, the downgoing radiation (4.6), is the probing of the Earth's atmosphere for trace gases by measuring their thermal radiation at GHz and THz frequencies (see, e.g., [5]). A variable sensitivity for different height ranges of the atmosphere is then achieved by tuning the spectrometer to frequencies at different distances to the center of a molecular rotational transition line. Hence, the method exploits the spectral variation in the absorption (or emission) coefficient κ_ν. We will therefore rewrite (4.6) for zenith observation ($|\cos\theta|$ = 1) and replace τ_ν again according to (4.3)

$$I_\nu^{\rm srf} = \int_0^\infty B_\nu(T(z))\ {\rm e}^{-\int_0^z \kappa_\nu(z')\,dz'}\,\kappa_\nu(z)\ dz$$

$$= \int_0^\infty B_\nu(T(z))\,\frac{d\mathcal{A}_\nu}{dz}\,dz \quad \text{where} \quad \mathcal{A}_\nu(z) = 1 - {\rm e}^{-\int_0^z \kappa_\nu(z')\,dz'} \tag{4.8}$$

$$\longrightarrow \int_0^\infty B_\nu(T(z))\ \kappa_\nu(z)\ dz \quad \text{if optically thin} \tag{4.9}$$

In (4.8), $\mathcal{A}_\nu$ is the attenuation at frequency ν between the Earth's surface and height z.

To simplify the analysis, we will restrict to a line which is optically thin, i.e., for which $\mathcal{A}_\nu(z)$ remains $\ll 1$ even for $z \to \infty$. This case is well approxiamted by (4.9). The absorpion coefficient κ_ν is a complicated expression and depends on the detailed physical process which leads to the absorption of the photon. For the inversion problem we only need to know its dependence on frequency ν, temperature T and density n_X of the molecular trace gas X under investigation. All other constants will be absorbed in a constant a. Consider a line at center frequency ν_{nm} = $(E_m - E_n)/h$ for a transition from state $n \to m$. Then (see, e.g., [6])

$$\kappa_\nu = a\, n_{X,n}\, \nu \Psi(\nu - \nu_{nm})\,(1 - \mathrm{e}^{-\frac{E_m - E_n}{k_B T}}) \tag{4.10}$$

The last factor includes the correction for induced emission, which is not negligible for energies in the IR range and below where $E_m - E_n \simeq k_B T$ or even less. $n_{X,n}$ is the number of X molecules in the lower state n which in thermal equilibrium can be expressed by the gas density n_{air}, the relative concentration c_X of the constituent X and relative number of them in state n

$$n_{X,n} = n_{\text{air}}\, c_X\, \frac{g_n \mathrm{e}^{-\frac{E_n}{k_B T}}}{Z(T)} \tag{4.11}$$

Here, g_n is the degeneracy of state n and $Z(T)$ is the partition function. The frequency dependence is expressed in the line shape function $\Psi(\nu - \nu_{nm})$ which for a large part of the Earth's atmosphere is dominated by the collisional broadening. The shape is well modelled by a Lorentzian line profile

$$\nu \Psi(\nu - \nu_{nm}) \simeq \nu_{nm} \Psi(\nu - \nu_{nm}) = \frac{\nu_{nm} \Delta\nu_C}{(\nu - \nu_{nm})^2 + (\Delta\nu_C)^2} \tag{4.12}$$

of width $\Delta\nu_C \ll \nu_{nm}$. In the atmosphere, the linewidth $\Delta\nu_C$ is essentially proportional to the ambient gas pressure (we neglect a minor temperature dependence)

$$\Delta\nu_C = \Delta\nu_0 \frac{p}{p_0} \tag{4.13}$$

where the coefficients $\Delta\nu_0$, p_0 are usually determined experimentally.

If we insert (4.10) to (4.13) into (4.9) and concentrate the all temperature dependence in a function F_{nm}, we obtain finally after replacing n_{air} by $p/k_B T$ and ν_{nm} by $(E_n - E_m)/h$

$$\boxed{I_\nu^{\text{srf}} = \int_0^\infty F_{nm}(T(z))\; \frac{\left(\frac{p(z)}{p_0}\right)^2}{\left(\frac{\nu - \nu_{nm}}{\Delta\nu_0}\right)^2 + \left(\frac{p(z)}{p_0}\right)^2}\; c_X(z)\; dz} \tag{4.14}$$

where

$$F_{nm}(T) = \frac{a\, g_n p_0}{h \Delta\nu_C}\; B_{\nu_{nm}}(T)\, \frac{E_m - E_n}{k_B T} \frac{\mathrm{e}^{-\frac{E_n}{k_B T}} - \mathrm{e}^{-\frac{E_m}{k_B T}}}{Z(T)}$$

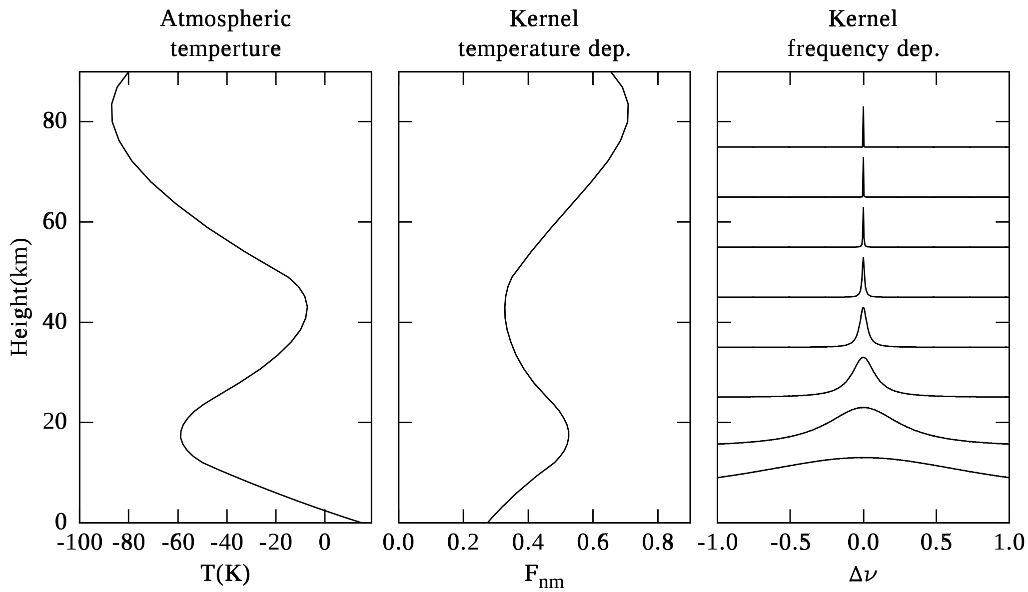

Figure 4: *Left panel: Typical temperature profile of the Earth's atmosphere. Central panel: Factor F_{nm} of (4.14) in arbitrary units. Right panel: Line shape function of kernel in (4.14) at various heights.*

The conventional procedure is to use (4.14) first with a molecular line of X = CO_2 or O to solve (4.14) for the temperature factor F_{nm}. These molecules are well mixed in the atmosphere up to about 100 km so that c_X is practically a constant. Once the temperature profile is known (4.14) can be used to retrieve the concentration c_X of other molecules like H_2O, O_3. The line shape factor varies between 1 at low heights (where at $\nu - \nu_{nm} \ll \Delta\nu_C$) and 0 at great heights (where at $\nu - \nu_{nm} \gg \Delta\nu_C$). The transition occurs at the height where $\nu - \nu_{nm} \simeq \Delta\nu_C \propto p(z)$. Hence varying $\nu - \nu_{nm}$ results in kernels of (4.14) which reach up to different heights. This allows to vary the kernel much more effectively than by the $1/\cos\theta$ factor in the limb darkening equation (4.7). The method can be used to find c_X up to heights where (4.12) is valid. For too small values of $\Delta\nu_C$ at heights above about 80 - 90 km the Doppershift of the thermal motion of the molecules eventually determines the width of the line rather than collisions. The line width then is no more pressure dependent and the kernel function consequently loses its height sensitivity.

5 Helioseismology

There are two different approaches in helioseismology. The first is to measure the travel times of acoustic waves by correlating Doppler data from different places on the solar surface and infer from it essentially the acoustic wave speed below the Sun's surface. The second approach analyses the eigenoscillations of the Sun and compares them with the eigenfrequencies calculated from standard solar models. With helioseismic inversion, discrepancies between the observed and calculated acoustic wave dispersion can directly be related to changes of the fluid parameters in the Sun's interior with respect to the standard model.

The approach is based on a variational principle which consists of the integration of the effect of small perturbations over the entire volume of the Sun. It is favourable to do this integration in terms of Lagrangian variables rather than using the conventional Euler variables of the fluid. The transformation of the equations of continuity, momentum and pressure to the Lagrangian frame is not trivial and is derived in appendix A. To simplify the matter, we will our considerations to a horizontally layered fluid with vertical gravity acceleration $\boldsymbol{g}(z)$. We count z positive upwards and $g = \hat{\boldsymbol{z}}\cdot\boldsymbol{g}$ is negative. This setting could be looked upon as an approximation for wave modes which do not propagate deeply into the interior of the Sun.

Hence, we assume that the background pressure p_0 and density ρ_0 depend only on depth z, are in hydrostatic equilibrium and g varies consistently with the density distribution

$$\nabla p_0 = \boldsymbol{g}\rho_0 \quad \text{and} \quad \nabla\cdot\boldsymbol{g} = -4\pi G\rho_0 \tag{5.1}$$

(5.1) can readily be integrated from the surface values $p_0(z = 0) = 0$ (negligible pressure from the corona) and $g(z = 0)$, which is the known gravitational acceleration on the Sun's surface.

The propagation of waves is controlled by three more z dependent background parameters, the acoustic speed, c_s, the Brunt-Vaisälä-frequency N and the pressure scale height H defined by

$$c_s^2 = \frac{\gamma p_0}{\rho_0} \tag{5.2}$$

$$N^2 = (-g)\left(\frac{\partial_z p_0}{\gamma p_0} - \frac{\partial_z \rho_0}{\rho_0}\right) = \frac{(-g)}{\gamma}\left(\frac{p_0}{\rho_0^\gamma}\right)^{-1}\frac{\partial}{\partial z}\left(\frac{p_0}{\rho_0^\gamma}\right) \tag{5.3}$$

$$H = \frac{p_0}{|g|\rho_0} = \frac{c_s^2}{\gamma|g|} \tag{5.4}$$

Both, c_s and H increase rapidly towards the Sun's interior. The Brunt-Vaisala frequency N is practically zero in the convection zone and only finite deep inside the Sun where it is stably layered. In (5.2)-(5.4), γ is the polytropic index (ratio of specific heats). We will assume for simplicity that it is a constant. In the real Sun, γ is considered to vary with depth due to changes in the chemical composition in its interior.

We assume a general perturbation expressed by the Lagrangian excursion $\boldsymbol{\xi}(\boldsymbol{x}_0, t)$ of a fluid element from its equilibrium location $\boldsymbol{x}_0$ (For convenience, we will drop the index 0 from $\boldsymbol{x}_0$ in the main text used in the appendices to denote the equilibrium position). As shown in appendix A, the perturbation obeys in linear approximation (see A.23)

$$\ddot{\boldsymbol{\xi}} = (\gamma - 1)\boldsymbol{g}(\nabla\cdot\boldsymbol{\xi}) + c_s^2\nabla(\nabla\cdot\boldsymbol{\xi}) + \nabla(\boldsymbol{g}\cdot\boldsymbol{\xi}) \equiv -\mathcal{A}(\boldsymbol{\xi}) \qquad (5.5)$$

This equation also neglects the gravitational effect of the density perturbations associated with (5.5), a common simplification termed Cowling approximation. The associated density and pressure perturbations are (A.13) and (A.16)

$$\delta_L\rho = -\rho_0\,(\nabla\cdot\boldsymbol{\xi}) \quad \text{and} \quad \delta_L p = -\gamma p_0\,(\nabla\cdot\boldsymbol{\xi}) \qquad (5.6)$$

As boundary conditions for the perturbation we demand that it should vanish deep in the interior at $z \to -\infty$ and at the surface and the pressure at the surface should stay zero, which requires that $(\nabla\cdot\boldsymbol{\xi})(z = 0) = 0$.

From the Doppler observations on the Sun's surface we obtain after Fourier transform in time and surface coordinates the frequency ω and horizontal wavenumber $\boldsymbol{k}_h$ of the perturbations. Consequently, we will decompose

$$\boldsymbol{\xi}(\boldsymbol{x}, t) = \sum_{\boldsymbol{k}_h,\omega} \boldsymbol{\xi}_{\boldsymbol{k}_h,\omega}(z)\, e^{i(\boldsymbol{k}_h\boldsymbol{x} - \omega t)} + c.c. \qquad (5.7)$$

and similarly for $\delta_L\rho$ and $\delta_L p$. Equations similar to (5.5) and (5.6) but with additional terms also hold in the more general case when selfgravitation is taken account of or if magnetohydrodynamic fluid forces are allowed for.

5.1 Approximation of short vertical wavelengths

As also shown in the appendix, (5.5) describes acoustic and gravity waves. The former are associated with pressure variations or according to (5.6) with $\mathrm{div}\boldsymbol{\xi}$, the latter with a vertical displacement ξ_z of the fluid parcels against gravity. The respective wave equations for vertical wavelengths short compared to the vertical scale height H are

$$\mathrm{div}\ddot{\boldsymbol{\xi}} - c_s^2\Delta\mathrm{div}\boldsymbol{\xi} \simeq 0 \quad \text{and} \quad \Delta\ddot{\xi}_z + N^2\Delta_h\xi_z \simeq 0 \qquad (5.8)$$

The boundary constraints which we impose on the perturbations is that they do not produce any pressure change at the surface $z = 0$ so that the total pressure is $p_0(z = 0) = 0$ and that all perturbations vanish for $z \to -\infty$.

This approximation is not meaningful for gravity waves. From (5.8) and (5.7) including a Fourier transform with respect to z (since $Hk_z \gg 1$ we can neglect the z dependence of N^2) we find a dispersion

$$k_z^2(z) \simeq \left(\frac{N^2(z)}{\omega^2} - 1\right) k_h \tag{5.9}$$

An increase of N^2 with depth causes the vertical wavenumber k_z to increase too, hence gravity waves tend to be deflected downwards towards the center of the Sun and $\xi_z(z) \to 0$ for $z \to -\infty$. The convection zone with $N \simeq 0$ in addition prevents them to reach the surface so that they are hard to detect at the surface (Up to now the so-called g-modes are still unobserved). In our simplified geometry we therefore have to rule out gravity waves in order not to get in conflict with the integrability of the wave functions and the boundary conditions for $\boldsymbol{\xi}$ demanded above.

For acoustic waves the above approximation makes sense. Their dispersion from (5.8) after Fourier transform in space and time is (again valid only for $Hk_z \gg 1$)

$$k_z^2(z) \simeq \frac{\omega^2}{c_s^2(z)} - k_h^2 \tag{5.10}$$

hence for increasing $c_s^2(z)$ with $-z$ the vertical wavenumber k_z decreases to zero where the wave is reflected upwards again. If the number of nodes of the wave in vertical direction is n then the integration of the waves' phase change in vertical direction yields

$$\int_{z_{\rm rfl}}^{0} k_z(z)\ dz = (n + \alpha_{\rm rfl} + \alpha_0)\pi \tag{5.11}$$

where $\alpha_{\rm rfl}$ and α_0 are phase corrections which depend on the specific reflection conditions at $z = z_{\rm rfl}$ and $z = 0$, but not on wavenumber or frequency. Experimentally, a value $\alpha_{\rm rfl} + \alpha_0 = 1.45$ is found [10].

Using (5.2) and (5.3), we can roughly estimate how c_s increases with depth, at least inside the convection zone. With $N^2 \simeq 0$,

$$\frac{1}{c_s^2}\frac{dc_s^2}{dz} = \left(\frac{1}{p_0}\frac{dp_0}{dz} - \frac{1}{\rho_0}\frac{d\rho_0}{dz}\right)$$
$$= \left(\frac{1}{p_0}\frac{dp_0}{dz} - \frac{1}{\gamma p_0}\frac{dp_0}{dz}\right) = (1 - \frac{1}{\gamma})\frac{g\rho_0}{p_0} = (\gamma - 1)\frac{g}{c_s^2}$$

We can use this equation to rewrite the dispersion (5.10) as

$$k_z^2(z) \simeq \frac{\omega^2}{(\gamma - 1)gz} - k_h^2$$

(Note, both g and z are negative), and insert this result into (5.11)

$$\int_{z_{\rm rfl}}^{0} \sqrt{\frac{\omega^2}{(\gamma-1)gz} - k_h^2}\; dz$$
$$= k_h|z_{\rm rfl}| \int_0^1 \sqrt{x^{-1}-1}\, dx = k_h|z_{\rm rfl}|\frac{\pi}{2} = (n+\alpha_{\rm rfl}+\alpha_0)\pi$$

where $z_{\rm rfl} = (\omega/k_h)^2/(\gamma-1)g$. The last equation yields the observable relation between the frequency and horizontal wavenumber

$$\omega^2 = \omega^2_{\boldsymbol{k}_h,n} \simeq 2(\gamma-1)g\,(n+\alpha_{\rm rfl}+\alpha_0)k_h \tag{5.13}$$

Therefore not all frequencies ω originally allowed for in (5.7) are possible, but only a discrete set labeled with $n \in \{0\} \cup \mathbb{N}$. Hence we should see a large number of modes n with similar dispersion curves. However, we can only hope this result to be even approximately valid as long as $z_{\rm rfl}$ lies inside the convection zone. Conversely, any observed deviation from (5.13) tells us that our guess about the fluid parameters inside the Sun have to be corrected.

5.2 The inverse problem from a variational princple

To find these corrections, we have to go back to (5.5) without restriction on the vertical wavelength. An essential requirement of the momentum equation (5.5) in a lossless system is that the differential operator $\mathcal{A}$ is selfadjoint with respect to ρ_0. In appendix B we show that this is indeed the case. For two perturbations $\boldsymbol{\xi}$ and $\boldsymbol{\zeta}$ we have (see B.10)

$$\int_{V_0} \rho_0 \boldsymbol{\zeta}\cdot\mathcal{A}(\boldsymbol{\xi})\; d^3\boldsymbol{x} = \int_{V_0} \rho_0 \boldsymbol{\xi}\cdot\mathcal{A}(\boldsymbol{\zeta})\; d^3\boldsymbol{x} = \int_{V_0} \rho_0 \mathcal{A}'(\boldsymbol{\zeta},\boldsymbol{\xi})\; d^3\boldsymbol{x} \tag{5.14}$$

where $\mathcal{A}'$ is a differential operator which is symmetric in both its arguments

$$\begin{aligned}\mathcal{A}'(\boldsymbol{\zeta},\boldsymbol{\xi}) = {} & \frac{\gamma p_0}{\rho_0}(\nabla\cdot\boldsymbol{\zeta})(\nabla\cdot\boldsymbol{\xi}) + \frac{1}{\rho_0}(\nabla\cdot\boldsymbol{\xi})(\boldsymbol{\zeta}\cdot\nabla p_0) \\ & + \frac{1}{\rho_0}(\nabla\cdot\boldsymbol{\zeta})(\boldsymbol{\xi}\cdot\nabla p_0) + \xi_z\zeta_z\frac{\partial_z\rho_0\,\partial_z p_0}{\rho_0^2}\end{aligned} \tag{5.15}$$

If we introduce the Fourier transform(5.7), $\mathcal{A}$ changes to $\mathcal{A}_{\boldsymbol{k}_h}$ where ∇ is replaced by $\partial_z + i\boldsymbol{k}_h$ when it acts on $\boldsymbol{\xi}$. As $\mathcal{A}$ is selfadjoint, $\mathcal{A}_{\boldsymbol{k}_h}$ is hermitian and hence possesses a series of orthogonal eigenvectors $\boldsymbol{\xi}_{\boldsymbol{k}_h}$ with real eigenvalues $\omega^2_{\boldsymbol{k}_h}$ for each $\boldsymbol{k}_h$. These are exactly the modes labeled with n in our simplified first approach above. In terms of these eigenvectors and eigenvalues we rewrite (5.5) as

$$\omega^2_{\boldsymbol{k}_h,n}\boldsymbol{\xi}_{\boldsymbol{k}_h,n} = \mathcal{A}_{\boldsymbol{k}_h}(\boldsymbol{\xi}_{\boldsymbol{k}_h,n}) \tag{5.16}$$

which is an ordinary differential equation in z. It becomes a Sturm-Liouville eigenvalue problem if the boundary conditions for $\boldsymbol{\xi}_{\boldsymbol{k}_h,n}$ are taken account of (see text following 5.5).

The orthogonality condition for these eigenvectors is

$$\int_{-\infty}^{0} \rho_0\, \boldsymbol{\xi}^*_{\boldsymbol{k}_h,m}(z)\boldsymbol{\xi}_{\boldsymbol{k}_h,n}(z)\; dz = \delta_{m,n}M_{\boldsymbol{k}_h,n} \tag{5.17}$$

where $M_{\boldsymbol{k}_h,n}$ is the normalization constant sometimes called the mode inertia. Likewise, (5.14) with the help of (5.16) can be rewritten as

$$\begin{aligned}\omega^2_{\boldsymbol{k}_h,n}M_{\boldsymbol{k}_h,n} &= \int_{-\infty}^{0} \rho_0\, \boldsymbol{\xi}^*_{\boldsymbol{k}_h,n}\cdot\mathcal{A}_{\boldsymbol{k}_h}(\boldsymbol{\xi}_{\boldsymbol{k}_h,n})\; dz \\ &= \int_{-\infty}^{0} \rho_0\mathcal{A}'_{\boldsymbol{k}_h}(\boldsymbol{\xi}^*_{\boldsymbol{k}_h,n}, \boldsymbol{\xi}_{\boldsymbol{k}_h,n})\; dz \end{aligned} \tag{5.18}$$

The operator $\mathcal{A}'_{\boldsymbol{k}_h}$ is identical to (5.15) except that ∇ is replaced by $\hat{\boldsymbol{z}}\partial_z \mp i\boldsymbol{k}_h$ where it operates onto the first or second argument of $\mathcal{A}'_{\boldsymbol{k}_h}$, respectively.

The eigenvectors of (5.16) form the elements of a Hilbertspace and the technique to correct the eigenvalues and eigenvectors due to changes in the operator $\mathcal{A}'_{\boldsymbol{k}_h}$ are borrowed from perturbation theory developed in quantum mechanics. The changes of $\mathcal{A}'_{\boldsymbol{k}_h}$ are due to corrections in the background quantities ρ_0, p_0, g which appear as coefficients in the operator. However, due to (5.1) ρ_0, p_0, g are not independent. Hence it is sufficient to only vary ρ_0 independently and take account of changes in the other background parameters in a consistent manner. These changes will induce a perturbation of the operator $\mathcal{A}_{\boldsymbol{k}_h}$ and finally further changes of the eigenvectors and eigenvalues

$$\begin{aligned}\mathcal{A}_{\boldsymbol{k}_h} &\to \mathcal{A}_{\boldsymbol{k}_h} + \delta\mathcal{A}_{\boldsymbol{k}_h} \\ \boldsymbol{\xi}_{\boldsymbol{k}_h,n} &\to \boldsymbol{\xi}_{\boldsymbol{k}_h,n} + \delta\boldsymbol{\xi}_{\boldsymbol{k}_h,n} \\ \omega^2_{\boldsymbol{k}_h,n} &\to \omega^2_{\boldsymbol{k}_h,n} + \delta(\omega^2_{\boldsymbol{k}_h,n})\end{aligned}$$

The correction to the eigenfunctions can be expressed as a combination of the unperturbed functions (Note, the $\boldsymbol{\xi}_{\boldsymbol{k}_h,n}$, are in general complete but we here ignore the gravity waves in our simplified treatment)

$$\delta\boldsymbol{\xi}_{\boldsymbol{k}_h,n} = \sum_m a_{n,m}\boldsymbol{\xi}_{\boldsymbol{k}_h,m} \tag{5.19}$$

The free constant of the perturbeded eigenfunctions are chosen such that the normalization (5.17) is maintained and $M_{\boldsymbol{k}_h}$ remains unaffected. As is easily seen when $\boldsymbol{\xi}_{\boldsymbol{k},n} \rightarrow \boldsymbol{\xi}_{\boldsymbol{k},n}$ + $\delta\boldsymbol{\xi}_{\boldsymbol{k},n}$ with (5.19) are inserted into (5.17), $a_{n,n} + a^*_{n,n}$ must vanish. The free complex phase of the pertubed eigenvector is chosen to make $a_{n,n}$ vanish entirely so that

$$\int_{-\infty}^{0} \rho_0 \, \delta\boldsymbol{\xi}^*_{\boldsymbol{k}_h,n} \cdot \boldsymbol{\xi}_{\boldsymbol{k}_h,n} \, dz = 0 \tag{5.20}$$

A variation of (5.16) then yields with (5.19), $a_{n,n}$ = 0 and also taking account of the linearity of the operator $\mathcal{A}_{\boldsymbol{k}_h}$

$$\begin{aligned}
\delta(\omega^2_{\boldsymbol{k}_h,n})\boldsymbol{\xi}_{\boldsymbol{k}_h,n} + \omega^2_{\boldsymbol{k}_h,n}\delta\boldsymbol{\xi}_{\boldsymbol{k}_h,n} &= \delta\mathcal{A}_{\boldsymbol{k}_h}(\boldsymbol{\xi}_{\boldsymbol{k}_h,n}) + \mathcal{A}_{\boldsymbol{k}_h}(\delta\boldsymbol{\xi}_{\boldsymbol{k}_h,n}) \\
&= \delta\mathcal{A}_{\boldsymbol{k}_h}(\boldsymbol{\xi}_{\boldsymbol{k}_h,n}) + \sum_{m\neq n} a_{n,m}\mathcal{A}_{\boldsymbol{k}_h}(\boldsymbol{\xi}_{\boldsymbol{k}_h,m}) \\
&= \delta\mathcal{A}_{\boldsymbol{k}_h}(\boldsymbol{\xi}_{\boldsymbol{k}_h,n}) + \sum_{m\neq n} a_{\,n,m}\omega^2_{\boldsymbol{k}_h,m}\boldsymbol{\xi}_{\boldsymbol{k}_h,m}
\end{aligned} \tag{5.21}$$

Multiplication with $\rho_0 \; \boldsymbol{\xi}^*_{\boldsymbol{k}_h,n}$ with (5.19) and (5.17) gives

$$\begin{aligned}
\delta(\omega^2_{\boldsymbol{k}_h,n})M_{\boldsymbol{k}_h,n} &= \int_{-\infty}^{0} \rho_0 \, \boldsymbol{\xi}^*_{\boldsymbol{k}_h,n} \cdot \delta\mathcal{A}_{\boldsymbol{k}_h}(\boldsymbol{\xi}_{\boldsymbol{k}_h,n}) \\
&= \int_{-\infty}^{0} \rho_0 \, \delta\mathcal{A}'_{\boldsymbol{k}_h}(\boldsymbol{\xi}^*_{\boldsymbol{k}_h,n}, \boldsymbol{\xi}_{\boldsymbol{k}_h,n}) \, dz
\end{aligned} \tag{5.22}$$

Hence the variation of the eigenvalue is obtained from the variation of the operator elements with respect to the unperturbed eigenfunctions. The perturbed eigenfunctions are not required at all at this approximation.

The density variation leads to a pertubation operator $\delta\mathcal{A}'_{\boldsymbol{k}_h}/\delta\rho_0$, actually the Fréchet derivative of $\mathcal{A}'_{\boldsymbol{k}_h}$, which we derive in the appendix C. This operator is again a Hilbert space operator as $\mathcal{A}'_{\boldsymbol{k}_h}$ itself. Our final inverse problem can now be stated in terms of new operator (5.22) as

$$\boxed{\frac{\delta(\omega^2_{\boldsymbol{k}_h,n})}{\omega^2_{\boldsymbol{k}_h,n}} = \int_{-\infty}^{0} \mathcal{K}_{\boldsymbol{k}_h}(\boldsymbol{\xi}^*_{\boldsymbol{k}_h,n}, \boldsymbol{\xi}_{\boldsymbol{k}_h,n})\frac{\delta\rho_0}{\rho_0} \, dz} \tag{5.23}$$

where we defined the kernel operator in accordance with the helioseismic literature [8] by

$$\mathcal{K}_{\boldsymbol{k}_h}(\boldsymbol{\xi}^*_{\boldsymbol{k}_h,n}, \boldsymbol{\xi}_{\boldsymbol{k}_h,n}) = \frac{\rho_0^2}{M_{\boldsymbol{k}_h,n}\omega^2_{\boldsymbol{k}_h,n}} \left(\frac{\delta\mathcal{A}'_{\boldsymbol{k}_h}}{\delta\rho_0}\right)(\boldsymbol{\xi}^*_{\boldsymbol{k}_h,n}, \boldsymbol{\xi}_{\boldsymbol{k}_h,n}) \tag{5.24}$$

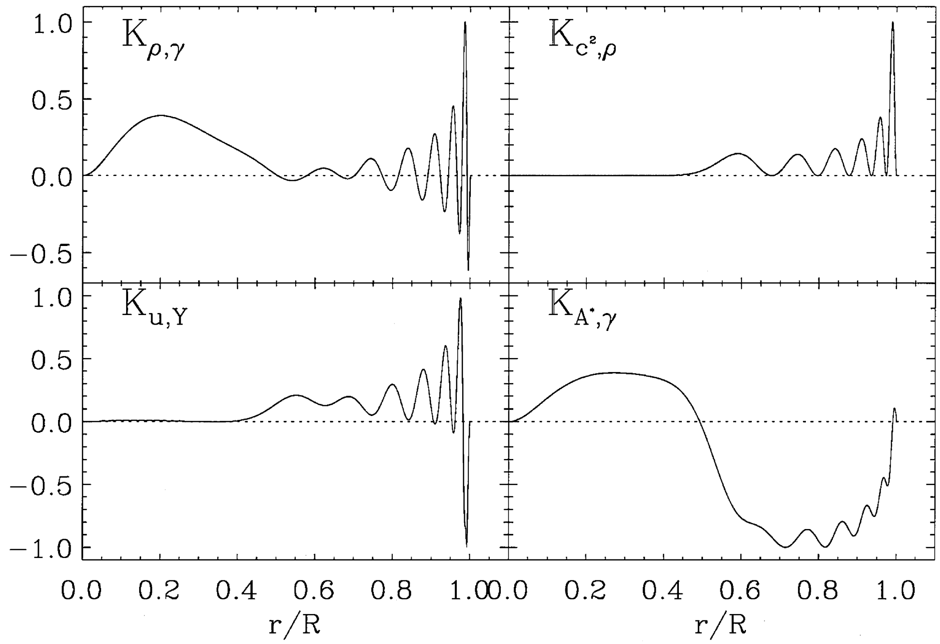

Figure 5: *Kernel functions $K_{\boldsymbol{k}_h}$ for an acoustic mode for the Sun, for spherical geometry so that $\boldsymbol{k}_h$ has to be replaced by $\sqrt{l(l+1)}/R_\odot$. Here, l = 10 and the eigenfunctions have the order n = 6. The first subscript parameter denotes the parameter which is varied, the second the one assumed fixed. Here, $u = c_s^2/\gamma$, A^* is essentially a measure of $N^2/|g|$ and Y is the relative Helium abundance. From [8].*

In (5.23) $\delta(\omega^2_{\boldsymbol{k}_h,n})$ is the deviation between the observed frequencies and those calculated from a standard solar model. Hence before solving (5.23), we must calculate the eigenfrequencies and eigenfunctions for the standard model from the unperturbed wave equation (5.16). The eigenvectors have to be used to calculate the kernel functions and the squared eigenfrequencies have to be subtracted from those observed to obtain $\delta(\omega^2_{\boldsymbol{k}_h,n})$ on the left hand side. The inversion of (5.23) then yields $\delta\rho_0$, the correction which we have to apply to our standard model (including consistent changes in p_0, g etc.) to obtain a better agreement between the observed and the model eigenfrequencies. A solution to (5.23) is made difficult by the fact that the kernel $\mathcal{K}$ is strongly influenced by the eigenfunctions $\boldsymbol{\xi}$ and oscillates heavily (see Fig. 5). Also a specific kernel only covers the depth range between the surface and the reflection height of the respective mode so that it is insensitive to density changes below the reflection height.

A Fluid equations in Lagrange variables

Be $\boldsymbol{x}_0$ the unperturbed location of a fluid element and $\boldsymbol{x}_0 + \boldsymbol{\xi}(\boldsymbol{x}_0, t)$ its perturbed location. In principle, $\boldsymbol{x}_0$ may be floating with a zero order background flow, but we will for simplicity restrict the unperturbed state to a stationary, vertically layered fluid in hydrostatic equilibrium. Moreover, we assume $\boldsymbol{\xi}$ small and will linearize with respect to $\boldsymbol{\xi}$. The relation between Euler coordinates $\boldsymbol{x}$ and the Largrangian equivalent is then

$$\boldsymbol{x} = \boldsymbol{x}_0 + \boldsymbol{\xi}(\boldsymbol{x}_0, t) \tag{A.1}$$

For a general variable F , we denote the unperturbed state by $F_0(\boldsymbol{x})$ which in our case is assumed stationary. The temporal evolution of the Eulerian perturbation of F is always measured at a fixed location $\boldsymbol{x}$ and we denote it by [9]

$$\delta_E F(\boldsymbol{x}, t) = F(\boldsymbol{x}, t) - F_0(\boldsymbol{x}) \tag{A.2}$$

In the Lagrangian frame, the temporal evolution of F is measured in the frame of reference floating with a fluid particle. We denote the respective perturbation by

$$\delta_L F(\boldsymbol{x}_0, \boldsymbol{\xi}(\boldsymbol{x}_0, t), t) = F(\boldsymbol{x}_0 + \boldsymbol{\xi}(\boldsymbol{x}_0, t), t) - F_0(\boldsymbol{x}_0) \tag{A.3}$$

If $\boldsymbol{x}$ is chosen according to (A.1), then obviously, $F(\boldsymbol{x}, t) = F(\boldsymbol{x}_0 + \boldsymbol{\xi}, t)$ and to lowest order,

$$\delta_L F(\boldsymbol{x}_0, \boldsymbol{\xi}(\boldsymbol{x}_0, t), t) = \delta_E F(\boldsymbol{x}_0, t) + \boldsymbol{\xi}(\boldsymbol{x}_0, t) \cdot \nabla F_0(\boldsymbol{x}_0, t) \tag{A.4}$$

An integral over a volume $V(t)$ whose boundary floats with the perturbed fluid transforms from Euler to Largrangian coordinates according to

$$\begin{aligned} &\int_{V(t)} F(\boldsymbol{x}, t)\ d^3\boldsymbol{x} = \\ &\int_{V_0} F(\boldsymbol{x}_0 + \boldsymbol{\xi}(\boldsymbol{x}_0, t), t) \det \left| \frac{\partial(\boldsymbol{x}_0 + \boldsymbol{\xi}(\boldsymbol{x}_0, t))}{\partial(\boldsymbol{x}_0)} \right|\ d^3\boldsymbol{x}_0 \end{aligned} \tag{A.5}$$

where the Lagrangian integration volume V_0 is the unperturbed volume which maps to $V(t)$ under (A.1). The determinant in (A.5) is the Jacobian of the transformation (A.1) and compensates the change of the infinitesimal volume element due to the mapping (A.1). The Jacobian can be simplified if we linearize

$$\begin{aligned} \det \left| \frac{\partial(\boldsymbol{x}_0 + \boldsymbol{\xi}(\boldsymbol{x}_0, t))}{\partial(\boldsymbol{x}_0)} \right| &= \det \left| \mathbf{1} + \frac{\partial(\boldsymbol{\xi}(\boldsymbol{x}_0, t))}{\partial(\boldsymbol{x}_0)} \right| \\ \simeq 1 + \mathrm{trace} \left(\frac{\partial(\boldsymbol{\xi}(\boldsymbol{x}_0, t))}{\partial(\boldsymbol{x}_0)} \right) &= 1 + (\nabla \cdot \boldsymbol{\xi})(\boldsymbol{x}_0, t) \end{aligned} \tag{A.6}$$

The integral in Euler coordinates is much more difficult because the boundaries are time dependent. We therefore transform the integrand to Lagrangian coordinates. The fluid (Euler) equations in Euler variables are

$$\left(\frac{d}{dt}\right)_E \rho = -\rho \nabla \cdot \boldsymbol{v} \tag{A.7}$$

$$\left(\frac{d}{dt}\right)_E \boldsymbol{v} = -\frac{1}{\rho} \nabla p + \boldsymbol{g} \tag{A.8}$$

$$\left(\frac{d}{dt}\right)_E p = -\gamma p \nabla \cdot \boldsymbol{v} \tag{A.9}$$

where

$$\left(\frac{d}{dt}\right)_E = \frac{\partial}{\partial t} + \boldsymbol{v}(\boldsymbol{x}, t) \cdot \nabla \tag{A.10}$$

is the convective derivative in Euler variables and we assume for simplification that $\boldsymbol{g}(z)$ is an unperturbed quantity in $\hat{\boldsymbol{z}}$ direction. This is equivalent to the Cowling approximation for spherical geometry and neglects the variations in the gravitational acceleration due to the density perturbations [10].

Equation (A.7) expresses the conservation of fluid mass in a convecting volume $V(t)$ compared to the unperturbed mass in V_0 at time $t = 0$ before the perturbation started. Hence we make use of (A.5) to express mass conservation in Largrangian coordinates:

$$\int_{V_0} \rho_0(\boldsymbol{x}_0)\; d^3\boldsymbol{x}_0 = \int_{V(t)} \rho(\boldsymbol{x}, t)\; d^3\boldsymbol{x}$$

$$= \int_{V_0} \rho(\boldsymbol{x}_0 + \boldsymbol{\xi}(\boldsymbol{x}_0, t), t) \det \left| \frac{\partial(\boldsymbol{x}_0 + \boldsymbol{\xi}(\boldsymbol{x}_0, t))}{\partial(\boldsymbol{x}_0)} \right| \; d^3\boldsymbol{x}_0 \tag{A.11}$$

Since V_0 was arbitrarily chosen, the last relation also holds for the integrands. Using (A.6)

$$\rho_0(\boldsymbol{x}_0) = \rho(\boldsymbol{x}_0 + \boldsymbol{\xi}(\boldsymbol{x}_0, t), t) \det \left| \frac{\partial(\boldsymbol{x}_0 + \boldsymbol{\xi}(\boldsymbol{x}_0, t))}{\partial(\boldsymbol{x}_0)} \right|$$

$$\simeq \rho(\boldsymbol{x}_0 + \boldsymbol{\xi}(\boldsymbol{x}_0, t), t)\, (1 + (\nabla \cdot \boldsymbol{\xi})(\boldsymbol{x}_0, t)) \tag{A.12}$$

The Lagrangian perturbation (A.3) of the density in lowest approximation is then

$$\delta_L \rho(\boldsymbol{x}_0, \boldsymbol{\xi}(\boldsymbol{x}_0, t), t) = \rho(\boldsymbol{x}_0 + \boldsymbol{\xi}(\boldsymbol{x}_0, t), t) - \rho_0(\boldsymbol{x}_0)$$

$$\simeq -\rho_0(\boldsymbol{x}_0)\, (\nabla \cdot \boldsymbol{\xi})(\boldsymbol{x}_0, t) \tag{A.13}$$

This result can simply be tranfered to any variable which depends only on denstiy

$$\delta_L F(\rho)(\boldsymbol{x}_0, \boldsymbol{\xi}(\boldsymbol{x}_0, t), t) = \frac{\partial F}{\partial \rho}(\rho_0(\boldsymbol{x}_0))\; \rho_0(\boldsymbol{x}_0)\, (\nabla \cdot \boldsymbol{\xi})(\boldsymbol{x}_0, t) \tag{A.14}$$

We will apply this relation to the pressure perturbation. From (A.9) and (A.7) we conclude that the fluid behaves adiabatically

$$\left(\frac{d}{dt}\right)_E \left(\frac{p}{\rho^\gamma}\right) = 0 \tag{A.15}$$

with the polytropic index γ, so that it can be considered to depend only on density ρ, i.e., $p \propto \rho^\gamma$. From (A.14) we find immediately

$$\delta_L p(\boldsymbol{x}_0, \boldsymbol{\xi}(\boldsymbol{x}_0, t), t) = -\gamma p_0(\boldsymbol{x}_0)\,(\nabla\cdot\boldsymbol{\xi})(\boldsymbol{x}_0, t) \tag{A.16}$$

If you compare (A.7) and (A.9) with their Lagrangian counterparts (A.13) and (A.16) you might be tempted to conclude that the transformation could be achieved formally by replacing essentially $(D/Dt)_E$ by δ_L. In fact,[9] show that these two operations commute under fairly general conditions. If we define $\boldsymbol{x}$ at a fixed time t by (A.1) then also $F(\boldsymbol{x}, t) = F(\boldsymbol{x}_0 + \boldsymbol{\xi}(\boldsymbol{x}_0, t), t)$ and especially,

$$\boldsymbol{v}(\boldsymbol{x}, t) = \boldsymbol{v}(\boldsymbol{x}_0 + \boldsymbol{\xi}(\boldsymbol{x}_0, t), t) = \dot{\boldsymbol{\xi}}(\boldsymbol{x}_0, t) \tag{A.17}$$

Hence, the convective derivative in Euler coordinates is exactly the full time dervative in Lagrangian coordinates (including the time dependence of $\boldsymbol{\xi}$)

$$\begin{gathered}\left(\frac{d}{dt}\right)_E F(\boldsymbol{x}, t) = \left(\frac{\partial}{\partial t}F + \boldsymbol{v}\cdot\nabla F\right)(\boldsymbol{x}, t) \\ = \left(\frac{\partial}{\partial t}F + \dot{\boldsymbol{\xi}}(\boldsymbol{x}_0, t)\cdot\nabla F\right)(\boldsymbol{x}_0 + \boldsymbol{\xi}(\boldsymbol{x}_0, t), t) = \frac{d}{dt}F(\boldsymbol{x}_0 + \boldsymbol{\xi}(\boldsymbol{x}_0, t), t)\end{gathered} \tag{A.18}$$

With these preliminaries we transform the momentum equation (A.8) to the Largrangian frame by formally applying δ_L to all terms. Using the fact that $\boldsymbol{v}_0$ = 0, (A.17) and (A.18).

$$\begin{gathered}\delta_L \left[\left(\frac{d}{dt}\right)_E \boldsymbol{v}\right](\boldsymbol{x}_0, \boldsymbol{\xi}(\boldsymbol{x}_0, t), t) \\ = \left[\left(\frac{d}{dt}\right)_E \boldsymbol{v}\right](\boldsymbol{x}_0 + \boldsymbol{\xi}(\boldsymbol{x}_0, t), t) - \underbrace{\left[\left(\frac{d}{dt}\right)_E \boldsymbol{v}_0\right]}_{0}(\boldsymbol{x}_0) \\ = \frac{d}{dt}\boldsymbol{v}(\boldsymbol{x}_0 + \boldsymbol{\xi}(\boldsymbol{x}_0, t), t) = \frac{d}{dt}\dot{\boldsymbol{\xi}}(\boldsymbol{x}_0, t) = \ddot{\boldsymbol{\xi}}(\boldsymbol{x}_0, t)\end{gathered} \tag{A.19}$$

and

$$\delta_L\left[\frac{1}{\rho}\nabla p\right](\boldsymbol{x}_0,\boldsymbol{\xi},t) \simeq -\frac{\nabla p_0}{\rho_0^2}\delta_L\rho(\boldsymbol{x}_0,\boldsymbol{\xi},t) + \frac{1}{\rho_0}\delta_L[\nabla p](\boldsymbol{x}_0,\boldsymbol{\xi},t)$$
$$= -\frac{\nabla p_0}{\rho_0^2}\delta_L\rho(\boldsymbol{x}_0,\boldsymbol{\xi},t) + \frac{1}{\rho_0}[(\nabla p)(\boldsymbol{x}_0+\boldsymbol{\xi},t) - (\nabla p_0)(\boldsymbol{x}_0)]$$
$$\simeq -\frac{\nabla p_0}{\rho_0^2}\delta_L\rho(\boldsymbol{x}_0,\boldsymbol{\xi},t) + \frac{1}{\rho_0}[\underbrace{(\nabla p)(\boldsymbol{x}_0,t) - (\nabla p_0)(\boldsymbol{x}_0)}_{\nabla[\underbrace{p(\boldsymbol{x}_0+\boldsymbol{\xi},t)-p_0(\boldsymbol{x}_0)}_{\delta_L p(\boldsymbol{x}_0,\boldsymbol{\xi},t)} - (\boldsymbol{\xi}\cdot\nabla)p_0(\boldsymbol{x}_0,t)]} + (\boldsymbol{\xi}\cdot\nabla)(\nabla p_0)(\boldsymbol{x}_0,t)]$$
$$= -\delta_L\rho\frac{\nabla p_0}{\rho_0^2}(\boldsymbol{x}_0,\boldsymbol{\xi},t) + \frac{1}{\rho_0}[\nabla\delta_L p(\boldsymbol{x}_0,\boldsymbol{\xi},t)\underbrace{-\nabla(\boldsymbol{\xi}\cdot\nabla p_0)(\boldsymbol{x}_0,t) + (\boldsymbol{\xi}\cdot\nabla)\nabla p_0(\boldsymbol{x}_0,t)}_{-\nabla(\xi_z\partial_z p_0) + \hat{\boldsymbol{z}}\xi_z\partial_z^2 p_0 \;=\; -\partial_z p_0\,\nabla\xi_z}]$$
$$= -\frac{\nabla p_0}{\rho_0^2}\delta_L\rho(\boldsymbol{x}_0,\boldsymbol{\xi},t) + \frac{1}{\rho_0}\nabla\delta_L p(\boldsymbol{x}_0,\boldsymbol{\xi},t) - \frac{1}{\rho_0}\partial_z p_0\,\nabla\xi_z(\boldsymbol{x}_0,t) \qquad \text{(A.20)}$$

As for $\boldsymbol{g}$, we want to neglect the gravitational effect due the density changes $\delta_L\rho$ (Cowling approximation), hence in the Euler frame $\boldsymbol{g}$ remains constant. In the Lagrangian frame, however, a perturbation is seen as a result of the inhomogeneity of $\boldsymbol{g}$ of

$$\delta_L[\boldsymbol{g}](\boldsymbol{x}_0,\boldsymbol{\xi},t) = \boldsymbol{g}(\boldsymbol{x}_0+\boldsymbol{\xi}) - \boldsymbol{g}(\boldsymbol{x}_0)$$
$$= (\boldsymbol{\xi}(\boldsymbol{x}_0,t)\cdot\nabla)\boldsymbol{g}(\boldsymbol{x}_0) = \hat{\boldsymbol{z}}\xi_z(\boldsymbol{x}_0,t)\,\partial_z(\frac{1}{\rho_0}\partial_z p_0)(\boldsymbol{x}_0) \qquad \text{(A.21)}$$

The final linearized form of the momentum equation in Lagrangian variables then is obtained by collecting the terms (A.19-A.21) with appropriate sign as in (A.8)

$$\ddot{\boldsymbol{\xi}}(\boldsymbol{x}_0,t) = \frac{\boldsymbol{g}}{\rho_0}\delta_L\rho(\boldsymbol{x}_0,\boldsymbol{\xi},t) - \frac{1}{\rho_0}\nabla\delta_L p(\boldsymbol{x}_0,\boldsymbol{\xi},t) + \nabla(\boldsymbol{g}\cdot\boldsymbol{\xi})(\boldsymbol{x}_0,t) \qquad \text{(A.22)}$$

where we used the hydrostatic equilibrium condition $\nabla p_0/\rho_0 = \boldsymbol{g}$. Another form of the momentum equation is obtained by expressing $\delta_L\rho$ and $\delta_L p$ with help of (A.13) and (A.16) in terms of $\boldsymbol{\xi}$ and abbreviating $\gamma p_0/\rho_0 = c_s^2$ for the acoustic speed

$$\ddot{\boldsymbol{\xi}}(\boldsymbol{x}_0,t) = (\gamma-1)\boldsymbol{g}(\nabla\cdot\boldsymbol{\xi})(\boldsymbol{x}_0,t) + c_s^2\nabla(\nabla\cdot\boldsymbol{\xi})(\boldsymbol{x}_0,t) + \nabla(\boldsymbol{g}\cdot\boldsymbol{\xi})(\boldsymbol{x}_0,t) \qquad \text{(A.23)}$$

Acoustic waves are immediately apparent in (A.23) by taking the divergence of (A.23)

$$\mathrm{div}\ddot{\boldsymbol{\xi}} - c_s^2\Delta\mathrm{div}\boldsymbol{\xi} \qquad \text{(A.24)}$$
$$= (\gamma-1)(\nabla\cdot\boldsymbol{g}\mathrm{div}\boldsymbol{\xi}) + \partial_z c_s^2\;\partial_z(\mathrm{div}\boldsymbol{\xi}) + \Delta(\boldsymbol{g}\cdot\boldsymbol{\xi})$$

The first and second term on the left describes the refraction of the acoustic wave in the stratified medium if the vertical wavelength approaches the pressure scale height H, the second term describes the coupling with gravity waves.

Gravity waves are more tideous to obtain. We start with (A.22) and replace $\delta_L \rho$ by the adiabatic relation $\rho_0 \delta_L p/\gamma p_0$ from (A.13) and (A.16) and use again $\nabla p_0/\rho_0 = \boldsymbol{g}$.

$$
\begin{aligned}
\ddot{\boldsymbol{\xi}} &= \frac{\nabla p_0}{\rho_0^2}\delta_L \rho - \nabla\left(\frac{\delta_L p}{\rho_0}\right) - \frac{\nabla \rho_0}{\rho_0^2}\delta_L p + \nabla(\boldsymbol{g}\cdot\boldsymbol{\xi}) \\
&= \left(\frac{\nabla p_0}{\gamma p_0} - \frac{\nabla \rho_0}{\rho_0}\right)\frac{\delta_L p}{\rho_0} - \nabla\left(\frac{\delta_L p}{\rho_0} - \boldsymbol{g}\cdot\boldsymbol{\xi}\right) \\
&= -\hat{\boldsymbol{z}}\frac{N^2}{g}\frac{\delta_L p}{\rho_0} - \nabla\left(\frac{\delta_L p}{\rho_0} - \boldsymbol{g}\cdot\boldsymbol{\xi}\right) \qquad \text{(A.25)}
\end{aligned}
$$

Note that $g < 0$. We use the horizontal and vertical components of this equation differently. On the horizontal components we operate the horizontal divergence ∇_h and solve for $\delta_L p/\rho_0$ to obtain

$$
\nabla_h^2\left(\frac{\delta_L p}{\rho_0}\right) = \nabla_h^2(\boldsymbol{g}\cdot\boldsymbol{\xi}) - \nabla_h \ddot{\xi}_h \qquad \text{(A.26)}
$$

On the vertical component of (A.25) we operate $\nabla_h^2 = \Delta_h$ and replace $\delta_L p/\rho_0$ from the equation (A.26) above

$$
\begin{aligned}
\Delta_h \ddot{\xi}_z &= -\left(\frac{N^2}{g} + \partial_z\right)\left(\Delta_h \frac{\delta_L p}{\rho_0}\right) + \partial_z \Delta_h(\boldsymbol{g}\cdot\boldsymbol{\xi}) \\
&= -\left(\frac{N^2}{g} + \partial_z\right)\left(\nabla_h^2(\boldsymbol{g}\cdot\boldsymbol{\xi}) - \nabla_h \ddot{\xi}_h\right) + \partial_z \Delta_h(\boldsymbol{g}\cdot\boldsymbol{\xi}) \\
&= \left(\frac{N^2}{g} + \partial_z\right)\nabla_h \ddot{\xi}_h - \frac{N^2}{g}\Delta_h(\boldsymbol{g}\cdot\boldsymbol{\xi}) \qquad \text{(A.27)}
\end{aligned}
$$

Finally, we replace $\nabla_h \ddot{\xi}_h$ by $\mathrm{div}\ddot{\boldsymbol{\xi}} - \partial_z \ddot{\xi}_z$ and rearrange terms in (A.27) to finally obtain

$$
\begin{aligned}
&\Delta \ddot{\xi}_z + N^2 \Delta_h \xi_z \qquad \text{(A.28)} \\
&= -\frac{N^2}{g}\left[\partial_z g\ \partial_z \xi_z + \partial_z\left(\xi_z \partial_z g\right) + \partial_z \ddot{\xi}_z\right] + \left(\frac{N^2}{g} + \partial_z\right)\mathrm{div}\ddot{\boldsymbol{\xi}}
\end{aligned}
$$

Again, the first term on the right describes the refraction of the gravity wave if the vertical wavelength becomes of the order of the H height of fluid. The last term is responsible for the coupling with acoustic waves (A.24) (A reformulation of (A.24) and (A.28) in terms of wave amplitudes $\nabla\cdot\rho_0\boldsymbol{\xi}$ and $\rho_0 \xi_z$ should eliminate the refraction term in both equations).

B Selfdjointness of $\mathcal{A}$

We rewrite (5.5), or likewise, (A.22 or A.23) slightly differently using $c_s^2 = \gamma p_0/\rho_0$ and $g = dp_0/dz$

$$\rho_0 \ddot{\boldsymbol{\xi}} = (\gamma - 1)\nabla \left[p_0 (\nabla \cdot \boldsymbol{\xi}) \right] + p_0 \nabla(\nabla \cdot \boldsymbol{\xi}) + \rho_0 \nabla(\boldsymbol{g} \cdot \boldsymbol{\xi}) = -\rho_0 \mathcal{A}(\boldsymbol{\xi}) \tag{B.1}$$

If $\boldsymbol{\zeta}$ is another perturbation vector satisfying the boundary condition then $\mathcal{A}$ is selfadjoint if

$$\int_{V_0} \rho_0 \boldsymbol{\zeta} \cdot \mathcal{A}(\boldsymbol{\xi})\; d^3\boldsymbol{x}_0 = \int_{V_0} \rho_0 \boldsymbol{\xi} \cdot \mathcal{A}(\boldsymbol{\zeta})\; d^3\boldsymbol{x}_0 \tag{B.2}$$

We insert (B.1) and show term by term that the integrand is symmetric in $\boldsymbol{\zeta}$ and $\boldsymbol{\xi}$ and hence they can be interchanged.

The first term of the right-hand side of (B.1) obviously gives a symmetric integrand. After partial integration

$$\begin{aligned} &\int_{V_0} (\gamma - 1)(\boldsymbol{\zeta} \cdot \nabla) \left[p_0 (\nabla \cdot \boldsymbol{\xi}) \right]\; d^3\boldsymbol{x}_0 \\ &= \int_{\partial V_0} (\gamma - 1) p_0 (\boldsymbol{\zeta} \cdot \hat{\boldsymbol{n}})(\nabla \cdot \boldsymbol{\xi})\; d^2\boldsymbol{x}_0 - \int_{V_0} (\gamma - 1) p_0 (\nabla \cdot \boldsymbol{\zeta})(\nabla \cdot \boldsymbol{\xi})\; d^3\boldsymbol{x}_0 \end{aligned} \tag{B.3}$$

where the surface integral vanishes because $p_0 = 0$ on the surface. Here $\hat{\boldsymbol{n}} = \hat{\boldsymbol{z}}$ is the surface normal vector of ∂V_0. For the second term of (B.1) we obtain after partial integration

$$\begin{aligned} &\int_{V_0} p_0 (\boldsymbol{\zeta} \cdot \nabla)(\nabla \cdot \boldsymbol{\xi})\; d^3\boldsymbol{x}_0 \\ &= \int_{\partial V_0} p_0 (\boldsymbol{\zeta} \cdot \nabla)(\hat{\boldsymbol{n}} \cdot \boldsymbol{\xi})\; d^2\boldsymbol{x}_0 - \int_{V_0} \left[\zeta_i\, \partial_i \xi_z\, \partial_z p_0 + p_0\, \partial_j \zeta_i\, \partial_i \xi_j \right]\; d^3\boldsymbol{x}_0 \\ &= -\int_{V_0} \left[g \rho_0 (\boldsymbol{\zeta} \cdot \nabla) \xi_z + p_0\, \partial_j \zeta_i\, \partial_i \xi_j \right]\; d^3\boldsymbol{x}_0 \end{aligned} \tag{B.4}$$

where again the surface term vanishes due to $p_0 = 0$. The only remaining nonsymmetric term, the first part of the integrand in the last integral is compensated by a similar term arising from the integration over the third term of (B.1)

$$\begin{aligned} &\int_{V_0} \rho_0 (\boldsymbol{\zeta} \cdot \nabla)(\boldsymbol{g} \cdot \boldsymbol{\xi})\; d^3\boldsymbol{x}_0 \\ &= \int_{V_0} \left[g \rho_0 (\boldsymbol{\zeta} \cdot \nabla) \xi_z + \rho_0\, \xi_z \zeta_z\, \partial_z g \right]\; d^3\boldsymbol{x}_0 \end{aligned} \tag{B.5}$$

Adding all terms (B.3) - (B.5) together, we can write the integral over the acceleration operator in the form proposed by [9]

$$\int_{V_0} \rho_0 \boldsymbol{\zeta}\cdot\mathcal{A}(\boldsymbol{\xi})\ d^3\boldsymbol{x}_0$$
$$= \int_{V_0} [(\gamma-1)p_0(\nabla\cdot\boldsymbol{\zeta})(\nabla\cdot\boldsymbol{\xi}) + p_0\,\partial_j\zeta_i\,\partial_i\xi_j\ - \rho_0\,\xi_z\zeta_z\,\partial_z g\,]\ d^3\boldsymbol{x}_0 \qquad \text{(B.6)}$$

In the helioseismic literature, however, another form of the operator is used, which seems to have been introduced first by [11]. It is found by changing the integral over the second term of (B.1) to

$$\int_{V_0} p_0(\boldsymbol{\zeta}\cdot\nabla)(\nabla\cdot\boldsymbol{\xi})\ d^3\boldsymbol{x}_0 = \int_{\partial V_0} p_0(\boldsymbol{\zeta}\cdot\hat{\boldsymbol{n}})(\nabla\cdot\boldsymbol{\xi})\ d^2\boldsymbol{x}_0$$
$$- \int_{V_0} (\boldsymbol{\zeta}\cdot\nabla p_0)(\nabla\cdot\boldsymbol{\xi}) + p_0(\nabla\cdot\boldsymbol{\zeta})(\nabla\cdot\boldsymbol{\xi})\ d^3\boldsymbol{x}_0 \qquad \text{(B.7)}$$

instead of (B.4). Again the surface integral vanishes because $p_0 = 0$. The integral over the third term of (B.1), expression (B.5), is further manipulated to

$$\int_{V_0} [\partial_z p_0\,(\boldsymbol{\zeta}\cdot\nabla)\xi_z + \rho_0\xi_z\zeta_z\,\partial_z g\,]\ d^3\boldsymbol{x}_0$$
$$= \int_{V_0} \left[(\boldsymbol{\zeta}\cdot\nabla)(\xi_z\partial_z p_0\,) - \xi_z\zeta_z\,\partial_z^2 p_0\ + \rho_0\xi_z\zeta_z\,\partial_z g\right]\ d^3\boldsymbol{x}_0$$
$$= \int_{\partial V_0} (\boldsymbol{\zeta}\cdot\hat{\boldsymbol{n}})\xi_z\partial_z p_0\ \ d^2\boldsymbol{x}_0$$
$$- \int_{V_0} \left[(\nabla\cdot\boldsymbol{\zeta})\xi_z\partial_z p_0\ + \xi_z\zeta_z\frac{\partial_z\rho_0\,\partial_z p_0}{\rho_0}\right]\ d^3\boldsymbol{x}_0 \qquad \text{(B.8)}$$

where we used

$$\rho_0\partial_z g\ - \partial_z^2 p_0\ = -\frac{\partial_z p_0\,\partial_z\rho_0}{\rho_0}$$

The surface integral in (B.8) vanishes because $\rho_0 = 0$ and hence $\partial_z p_0\ = g\rho_0$ vanishes at the surface. Collecting (B.3), (B.7) and (B.8) we find as alternative to (B.6)

$$\int_{V_0} \rho_0 \boldsymbol{\zeta}\cdot\mathcal{A}(\boldsymbol{\xi})\ d^3\boldsymbol{x}_0$$
$$= \int_{V_0} \left[\gamma p_0(\nabla\cdot\boldsymbol{\zeta})(\nabla\cdot\boldsymbol{\xi}) + (\nabla\cdot\boldsymbol{\xi})(\boldsymbol{\zeta}\cdot\nabla p_0)\right.$$
$$\left. +(\nabla\cdot\boldsymbol{\zeta})(\boldsymbol{\xi}\cdot\nabla p_0) + \xi_z\zeta_z\frac{\partial_z\rho_0\,\partial_z p_0}{\rho_0}\right]\ d^3\boldsymbol{x}_0 \qquad \text{(B.10)}$$

This representation of the acceleration operation has the advantage that differentiations are shifted onto the gently varying functions ρ_0 and p_0 rather than onto the heavily oscillating wave functions.

C Variational change of $\mathcal{A}'$

We derive here the variational expression for the operator $\mathcal{A}'$, as defined in (5.15). The respective variation of $\mathcal{A}'_{\boldsymbol{k}_h,n}$ is as usual obtained by setting $\nabla \to \boldsymbol{k}_h \pm \hat{\boldsymbol{z}}\partial_z$

First we write down how p_0 and g are affected by a variation $\delta\rho_0$. We assume that $g_\odot$ is the gravitational acceleration on the Sun's surface at $z = 0$ which is to stay constant. We we therefore allow only variations $\delta\rho_0$ for which $\int \delta\rho_0 = 0$, i.e. the mass is only redistributed. The reason for this constraint is that the total mass of the Sun is very well known from celestial mechanics and we don't want this parameter to be changed when solving the inverse problem. From (5.1)

$$p_0(z) = -\int_z^0 g\rho_0 \; dz \quad \text{and} \quad g(z) = g_\odot + 4\pi G \int_z^0 \rho_0 \; dz \tag{C.1}$$

(remember g and $g_\odot$ are negative) we obtain

$$\delta p_0 = -\int_z^0 (g\delta\rho_0 + \rho_0 \delta g) \; dz \quad \text{and}$$

$$\delta g = 4\pi G \int_z^0 \delta\rho_0 \; dz = -4\pi G \int_{-\infty}^z \delta\rho_0 \; dz \tag{C.2}$$

We can now attact the variation of the operator $\mathcal{A}'$

$$\delta\mathcal{A}'(\boldsymbol{\zeta},\boldsymbol{\xi}) = \gamma(\nabla\cdot\boldsymbol{\zeta})(\nabla\cdot\boldsymbol{\xi})\,\delta\Big(\frac{p_0}{\rho_0}\Big) + \big[(\nabla\cdot\boldsymbol{\xi})\zeta_z + (\nabla\cdot\boldsymbol{\zeta})\xi_z\big]\,\delta g + \xi_z\zeta_z\,\delta\Big(\frac{g\partial_z\rho_0}{\rho_0}\Big)$$

where

$$\delta\Big(\frac{p_0}{\rho_0}\Big) = \frac{\delta p_0}{\rho_0} - p_0\frac{\delta\rho_0}{\rho_0^2} \tag{C.3}$$

$$\delta\Big(\frac{g\partial_z\rho_0}{\rho_0}\Big) = \frac{\partial_z\rho_0}{\rho_0}\delta g + \frac{g}{\rho_0}\partial_z(\delta\rho_0) - \frac{g\partial_z\rho_0}{\rho_0^2}\delta\rho_0 \tag{C.4}$$

Insertion gives

$$\begin{aligned}\rho_0\delta\mathcal{A}'(\boldsymbol{\zeta},\boldsymbol{\xi}) = {} & \gamma(\nabla\cdot\boldsymbol{\zeta})(\nabla\cdot\boldsymbol{\xi})\,\Big(\delta p_0 - p_0\frac{\delta\rho_0}{\rho_0}\Big) + \big[(\nabla\cdot\boldsymbol{\xi})\zeta_z + (\nabla\cdot\boldsymbol{\zeta})\xi_z\big]\rho_0\,\delta g \\ & +\xi_z\zeta_z\,\Big(\partial_z\rho_0\,\delta g + g\partial_z(\delta\rho_0) - \frac{g\partial_z\rho_0}{\rho_0}\delta\rho_0\Big)\end{aligned} \tag{C.5}$$

which in (5.22) we have integrate over the entire domain.

In a final stage we want to remove the integration on $\delta\rho_0$ implicit in δp_0 and δg and also the differention on $\delta\rho_0$ so that we finally can separate $\delta\rho_0$ in the integrand and thus obtain a multiplicative kernel. This will be achieved by suitable partial integration. The term with $\partial_z(\delta\rho_0)$ gives

$$\int\limits_{-\infty}^{0} g\xi_z\zeta_z\,\partial_z(\delta\rho_0)\;dz = -\int\limits_{-\infty}^{0} \partial_z(g\xi_z\zeta_z)\,\delta\rho_0\,dz$$

where the contributions at the boundaries vanish because there $\delta\rho_0 = 0$. Terms with δp_0 for

$$A_1 = \gamma(\nabla\cdot\boldsymbol{\zeta})(\nabla\cdot\boldsymbol{\xi}) \quad \text{yield}$$

$$\begin{aligned}
\int\limits_{-\infty}^{0} A_1\delta p_0\;dz &= \int\limits_{-\infty}^{0} \partial_z\Big(\int_{-\infty}^{z} A_1(z')\,dz'\Big)\,\delta p_0\;dz \\
&= -\int\limits_{-\infty}^{0} \Big(\int_{-\infty}^{z} A_1(z')\,dz'\Big)\partial_z(\delta p_0)\;dz \\
&= -\int\limits_{-\infty}^{0} \Big(\int_{-\infty}^{z} A_1(z')\,dz'\Big)(g\delta\rho_0+\rho_0\delta g)\;dz
\end{aligned}$$

Similarly terms with δg for

$$A_2 = \rho_0\big[(\nabla\cdot\boldsymbol{\xi})\zeta_z+(\nabla\cdot\boldsymbol{\zeta})\xi_z\big]+\xi_z\zeta_z\partial_z\rho_0\;-\rho_0\int\limits_{-\infty}^{0}\Big(\int_{-\infty}^{z} A_1(z')\,dz'\Big) \quad \text{give}$$

$$\begin{aligned}
\int\limits_{-\infty}^{0} A_2\delta g\;dz &= -\int\limits_{-\infty}^{0} \Big(\int_{-\infty}^{z} A_2(z')\,dz'\Big)\partial_z(\delta g)\;dz \\
&= 4\pi G\int\limits_{-\infty}^{0} \Big(\int_{-\infty}^{z} A_2(z')\,dz'\Big)\delta\rho_0\;dz
\end{aligned}$$

In both cases the integral over coefficient A vanishes at $-\infty$ and δp_0 or δg, respectively, vanish at the upper integration boudary so that the boundaries do not contribute to the partial integration. Inserting these expressions with appropriate coefficients and reordering yields finally

$$\int_{-\infty}^{0} \rho_0 \delta\mathcal{A}'(\boldsymbol{\zeta},\boldsymbol{\xi})\, dz = \int_{-\infty}^{0} \rho_0 \Big(\frac{\delta\mathcal{A}'}{\delta\rho_0}\Big)(\boldsymbol{\zeta},\boldsymbol{\xi})\, \frac{\delta\rho_0}{\rho_0}\, dz \quad \text{where}$$

$$\rho_0\Big(\frac{\delta\mathcal{A}'}{\delta\rho_0}\Big) = \gamma\Big[(\nabla\cdot\boldsymbol{\zeta})(\nabla\cdot\boldsymbol{\xi})\int_z^0 g\rho_0 dz' - g\rho_0\int_{-\infty}^{z}(\nabla\cdot\boldsymbol{\zeta})(\nabla\cdot\boldsymbol{\xi})dz'\Big]$$
$$-\partial_z(g\rho_0\xi_z\zeta_z) + 4\pi G\rho_0\int_{-\infty}^{z} S\rho_0 dz' \tag{C.7}$$

with

$$S(z) = \big[(\nabla\cdot\boldsymbol{\xi})\zeta_z + (\nabla\cdot\boldsymbol{\zeta})\xi_z\big] + \xi_z\zeta_z\frac{\partial_z\rho_0}{\rho_0} - \gamma\int_{-\infty}^{z}(\nabla\cdot\boldsymbol{\zeta})(\nabla\cdot\boldsymbol{\xi})\, dz'$$

References

[1] D.C. Champeney, *Fourier transformations and their physical applications*, Academic Press, London (1973)

[2] F. Natterer, *The mathematics of computerized tomography*, John Wiley, Chicester (1986)

[3] A.C Kak and M. Slaney, *Principles of computerized tomographic imaging*, IEEE Press, New York (1987)

[4] D.S. Evans, *An analysis of the solar atmospheric structure*, Monthly Notes, **107** (1947) 433, (as referenced in [7])

[5] A.L. Fymat and V.E. Zuev (Edts.), *Remote sensing of the atmosphere - Inversion methods and applications*, Elsevier, Amsterdam (1979)

[6] H.R. Griem, *Principles of plasma spectroscopy*, Cambridge University Press, Cambridge (1997)

[7] A. Unsöld, *Physik der Sternatmosphären* Springer, Heidelberg (1968)

[8] A.G. Kosovichev, *Inversion methods in helioseimology and solar tomography*, J. Comp. Appl. Math. **109** (1999) 1-39

[9] D. Lynden-Bell and J.P. Ostriker, *On the stability of differentially rotating bodies*, Mon. Not. R. astr. Soc. **136** (1967) 293-310

[10] J. Christensen-Daalsgaard, *Lecture Notes on Stellar Oscillations*, 4th Edition (1998),
available in internet: `www.obs.aau.dk/~jcd/oscilnotes`

[11] S. Chandrasekhar, *A general variational principle governing the radial and non-radial oscillations of gaseous masses*, Astrophys. J. **138** (1963) 896-897